FISEVIER

Contents lists available at ScienceDirect

Climate Risk Management

journal homepage: www.elsevier.com/locate/crm





Performance of dry and wet spells combined with remote sensing indicators for crop yield prediction in Senegal

Cheikh Modou Noreyni Fall ^{a,*}, Christophe Lavaysse ^b, Hervé Kerdiles ^c, Mamadou Simina Dramé ^a, Philippe Roudier ^d, Amadou Thierno Gaye ^a

- a Laboratoire de Physique de l'Atmosphère et de l'Océan-Simeon Fongang, ESP, Univ. Cheikh Anta Diop, Fann, Dakar, Senegal
- ^b Institut des Géosciences de l'Environnement IGE, Univ. Grenoble Alpes, IRD, CNRS, Grenoble INP, 38000 Grenoble, France
- ^c European Commission Monitoring Agricultural Resources, Institute for Environment and Sustainabilty Ispra (VA), Italy
- ^d Innovation, Research and Knowledge Department, Agence Française de Développement, Paris, France

ARTICLE INFO

Keywords: Dry/Wet spells Remote sensing Crop yields Multiple linear regression model

ABSTRACT

Studying the relationship between potential high-impact precipitation and crop yields can help us understand the impact of the intensification of the hydrological cycle on agricultural production. The objective of this study is to analyse the contribution of intra seasonal rainfall indicators, namely dry and wet spells, for predicting millet yields at regional scale in Senegal using multiple linear regression. Using dry and wet spells with traditional indicators i.e. proxies of crop biomass and cumulated rainfall, hereafter called remote sensing indicators (NDVI, SPI3, WSI and RG), we analysed the ability of dry and wet spells alone or combined with these remote sensing indicators to provide intraseasonal forecasts covering the period 1991-2010. We analysed all 12 regions producing millet and found that results vary strongly between regions and also during the season, as a function of the dekad of prediction. At the spatial scale, the strongest performing combinations include the dry spell indicators DSC20 and DSxl in the peanut basin. While in the south of the country, the combination of wet period indicators WS1 or WSC5 with the RG is fairly reliable. Focussing on Thies, our best region in the groundnut basin, we showed that dry and wet spells indicators can explain up to 80% of yield variations, alone or in combination with remote sensing indicators. Regarding the timing of prediction, millet yield can be forecast as early as July with an accuracy of 40% of the mean yield but the best forecast is obtained in early September, at the peak of crop development (accuracy of 100 kg/ha i.e. 20% of the mean yield). Although, the estimated yields show biases over some years identified as extremely deficient or in oversupply in terms of agricultural yields.

1. Introduction

Increasing occurrence of extreme events, coupled with a growing population is threatening food security in Sahelian countries (Meehl et al., 2000; Lebel and Ali, 2009; Alhassane et al., 2013; Panthou et al., 2014; Giannini, 2015; Descroix et al., 2016; Taylor et al., 1982; Panthou et al., 2018; Wilcox et al., 2018; Young et al., 2019). In these countries and in particular Senegal, agriculture is the main source of employment with nearly 60% of the population's livelihoods being dependent on agriculture (Dieng et al., 2008; Sultan et al.,

E-mail address: cheikhnoreyni.fall@esp.sn (C.M.N. Fall).

https://doi.org/10.1016/j.crm.2021.100331

^{*} Corresponding author.

2013; Roudier et al., 2014). Extreme rainfall events, mainly droughts, reduce agricultural productivity and decimate livestock herds. Successive crop failures have led to food insecurity, malnutrition and ultimately famine with loss of human life (Rosenzweig et al., 2001; Ganyo et al., 2018; Lalou et al., 2019). Consequences of these high-impact rainfall events include increases in basic food prices, food imports and rural—urban migration (Lalou et al., 2019; Sultan and Gaetani, 2016). As a result of the 2018 drought, Senegal was one of seven Sahelian countries where the number of food-insecure people increased significantly from 314,600 to 548,000 during the 2018 lean season, (i.e. the period between planting and harvesting when food stocks are low and job opportunities are scarce, usually between June and August in Senegal (WFP, 2018)). Although, total seasonal rainfall is important, it does not characterize the intraseasonal distribution of rainfall, in other words the water available to crops during the season which plays a major role in crop growth and yield determination (Sivakumar, 1992; Barron et al., 2003).

The Sahel experienced extreme decadal variability in rainfall during the twentieth century, with severe droughts during the 1970s and 1980s following a wet period in the 1950s and 1960s. Since the late 1990s, rainfall has partly recovered to its climatology. Nevertheless this recovery of rainfall is accompanied by changes in the intra-seasonal time scale compared to the 1950s and 1960s (Taylor et al., 1982; Sane et al., 2018; Vischel et al., 2019). Indeed, rainfall during the season records nowadays more extreme hydrological conditions, with longer dry spells and more intense wet spells (Giorgi et al., 2011; Trenberth et al., 2003; Trenberth, 2011; Salack et al., 2016; Froidurot and Diedhiou, 2017; Panthou et al., 2018). In Senegal, heavy rainfall is caused by different synoptic systems which determine the duration of wet spells. Extreme wet spells (above the 99th percentile) are of particular concern as they often cause floods in the mid season. As for dry spells, showed that the more frequent long dry spells since the 1990s are often markers of false start and early cessation of the rainy season and therefore may impact crop production. The origins of these recent changes in wet and dry spells characteristics are not yet fully understood. The role of tropical Sea Surface Temperatures (SST) seems to be of lesser influence when compared with other identified drivers such as the intensification of the Saharan heat low (SHL; Lavaysse et al., 2016), the Mediterranean SST warming (Park et al., 2016), and the increase in atmospheric concentration of greenhouse gases (GHG; Dong and Sutton, 2015). These wet (dry) sequences in the West African monsoon (WAM) are associated with a westward propagation of cyclonic (anticyclonic) circulation in the wind field at 925 hPa consistent with positive (negative) rainfall anomalies over the Sahel and with a stronger (weaker) moisture advection over West Africa (Lavaysse et al., 2006). The origin of such fluctuations in the WAM and the interaction with synoptic disturbances such as African Easterly Waves (AEWs) are not well understood. AEWs are found on 3-5 and 6-9 days periodicity and can be associated to the Mesoscale convective systems (MCS) known to contribute to a large fraction of rain in West Africa (90%, Lebel et al., 2003; Jenkins et al., 2010; Lafore et al., 2017; Vischel et al., 2019.

Up to now, very few studies have analysed the impact of extreme dry and wet spells on agricultural yields in the Sahel, particularly in Senegal. In Mali, Sultan et al., 2009 has shown that the start and duration of the rainy season are major factors determining cotton productivity and its spatial distribution, although other non-climatic factors such as agricultural practices, biotic stresses (e.g. pests) also affect yield. In southern Senegal, Bacci (2017) evaluated the recurrence of drought and extreme rainfall conditions in the most sensitive phases of the rice crop cycle and identified trends in rainy season distribution over the period 1981–2013. Their analysis focused on the critical aspects that determine rice yield such as availability of water in the plant germination and flowering phases, and the dynamics of the rainy season. They identified the probability of extreme event occurrence during sensitive phases of rice crop development using the return period method. They found that in the last decade the favourable rainfall distribution in the initial phase of the growing season led to a low probability of unfavorable conditions for crops. In this study, we plan to investigate the relationships between millet yields and the occurrence of dry/wet spells defined in Fall et al. (2021).

The main methods to explore climate-yield relationships are either process-based crop models or statistical models. Process-based crop models simulate the growth of crops accounting for weather and soil factors, together with crop and management parameters. They aim to synthesize the understanding of crops' response to their environment (Rosenzweig et al., 2013). However, most process-based crop models perform poorly in handling the effects of extreme climate events on crop growth due to inaccurate descriptions of certain processes (Moriondo et al., 2011). Furthermore, crop models require several years of experimental data to train and calibrate to the local environment (Chen et al., 2004) and must be recalibrated for use in other regions; last, getting accurate data on management parameters (e.g. crop variety, sowing date, fertilisation) is difficult at the regional scale. Because of these limitations in these models, statistical models, such as multiple linear regression, have been widely used to relate crop yields with climate variables (Tebaldi and Lobell, 2008; Laudien et al., 2020) or even process-based crop models output variables (Nain et al., 2004; Lobell et al., 2030). Statistical models can be useful to predict crop yield despite not being directly based on the mechanisms that determine plant growth. The main advantages of statistical models are their limited reliance on field calibration data, and their transparent assessment of model uncertainties (Lobell and Burke, 2010). With the increasing availability and improved quality of observed data, statistical models usually perform well. Innes et al. (2015) suggested a superior performance of linear models in comparison with crop models to identify climate-vield relationships.

In this study we opted for an approach based on statistical models and selected CST (the Crop Statistics Tool), a freeware developed at the Joint Research Centre of the European Commission (JRC-EU) and used for predicting crop yields operationally every month over Europe (Kerdiles et al., 2017). We also took as yield predictors remote sensing indicators provided by ASAP (Anomaly Hotspots of Agricultural Production), the JRC early warning system for assessing agricultural drought globally (Rembold et al., 2018) to compare their performance with that of wet and dry spells indicators. The main objectives of this study were to (1) characterize the spatiotemporal variation of dry/wet spells and remote sensing indicators used (2), quantify the relationship of different combinations of dry/wet spells and remote sensing indicators with observed millet yields for the period 1991–2010, and (3) analyze the spatiotemporal variations of these relationships.

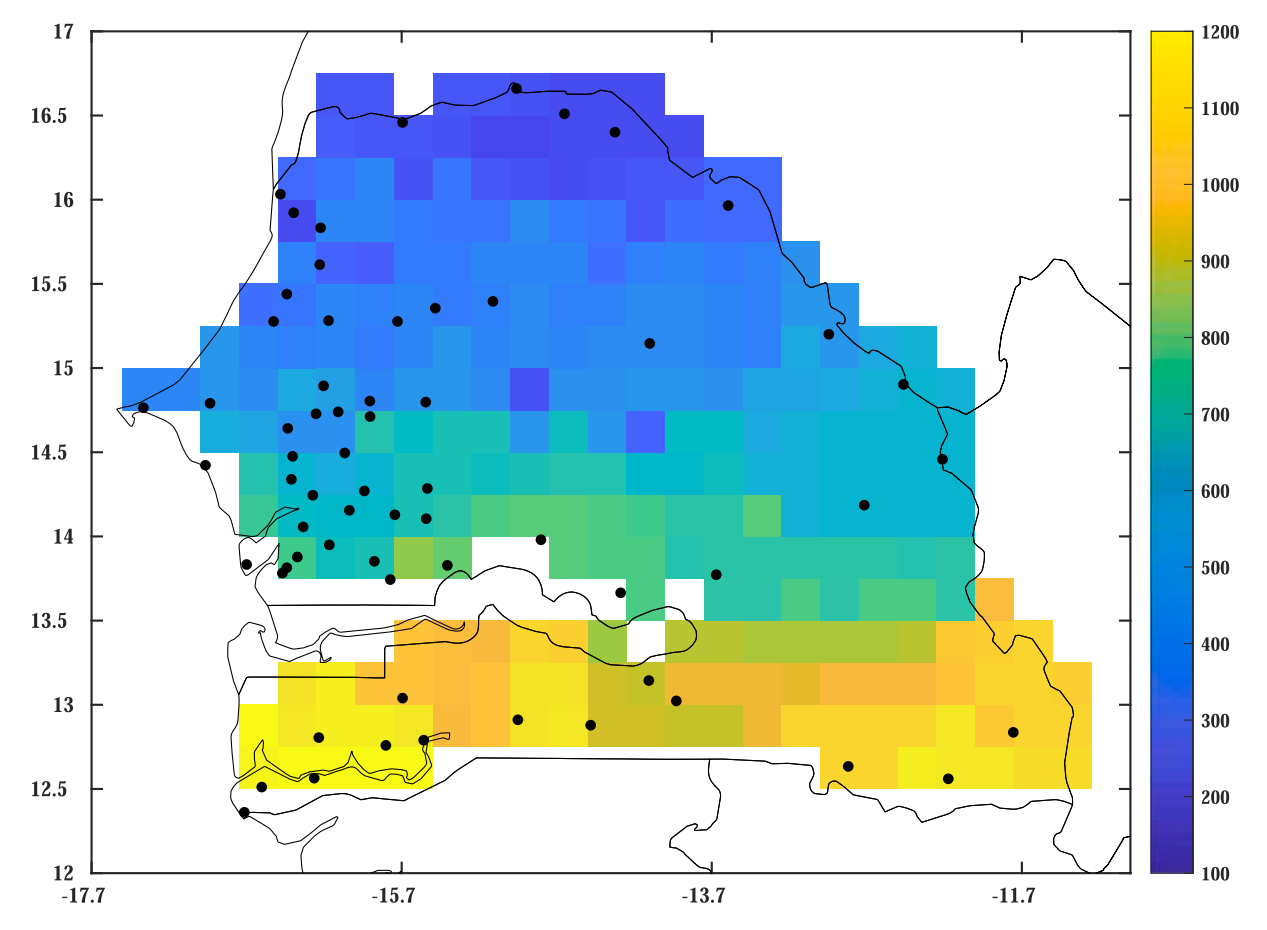


Fig. 1. The average cumulative precipitation over the period 1991-2010 is computed from daily rain-gauge data gridded by the block kriging (BK) method at $0.25^{\circ} \times 0.25^{\circ}$ as resolution. The black dots deNote 65 rain gauges of ANACIM used for this study to compute dry and wet spell indicators (Fall et al., 2021).

2. Study area

Located in West Africa, Senegal has a fairly flat landscape with altitudes below 50 m for more than 75% of its territory (196 722 km2). The climate of Senegal is governed by the WAM (Lafore et al., 2010; Janicot et al., 2011; Nicholson, 2013), resulting in a strong north-south gradient of the mean annual rainfall (See Fig. 1) ranging from 300 mm in the north to more than 1000 mm in the south (Diop et al., 2016; Sane et al., 2018). The rains are mainly caused by MCSs crossing the country from east to west (Laurent et al., 1998; Mathon et al., 2002; Diongue et al., 2002) but also by smaller systems such as isolated thunderstorms (Dione et al., 2014). WAM is also characterized by a strong intraseasonal variability with dry and wet spells over the Sahel (Lavaysse et al., 2006), whose consequences can be dramatic for socio-economic activities of the region. Although a comprehensive view of the WAM intraseasonal variability is still lacking, Janicot et al. (2011) identified the main modes of variability of the WAM at different intra seasonal time scales. They found that these modes have a regional extension and represent an envelope modulating the convective activity of individual systems. These modes are intermittent but their impact on precipitation and convective activity is strong when they occur. They have a marked zonal propagation character, westward for the Madden-Julian Oscillation (MJO, Lavender and Matthews, 2009; Pohl et al., 2009) and Sahel modes, and eastward for the Quasi-Biweekly Zonal Dipole (QBZD, Mounier et al., 2008) mode, although its stationary component is important over Africa. These modes are controlled both by internal atmospheric dynamics and land-surface interactions. At the synoptic scale, the MCSs are embedded within AEWs, synoptic perturbations of 3000-4000 km wavelength that propagate westward at 6-7 m.s⁻¹, and feed the MCSs with vorticity (Schwendike and Jones, 2010; Berry and Thorncroft, 2012) and humidity (Poan et al., 2015).

In this study we focused on millet, which is the main staple crop in the country, accounting for nearly 64% of total cereal production (Sultan and Gaetani, 2016). In Senegal farmers use adapted varieties (e.g. late or early millet) or adapt their practices (e.g. late or early sowing) according to the environment (Dingkuhn et al., 2006). The length of the vegetative cycle allows to classify the varieties into three main groups: The early "souna" varieties of 75 to 95 days are fairly common in the peanut basin, the semi-late "sanio" varieties of 110 to 130 days and the late photoperiodic varieties of 130 to 200 days, which are very common in the South (Sy et al., 2015). Millet is one of the most drought-tolerant crops among cereal species used as human food in the world. Millet is best adapted to light textured

soils with low annual rainfall (400–750 mm). In the peanut basin, planting always takes place during the dekad when rainfall has reached the minimum level for wet sowing (20 mm) in the case of groundnut and associated crops such as beans. In contrast, for millet, in most Senegal, a local village committee decides the sowing date before the rains start (Grillot, 2018). The exception to this rule is Upper Casamance, where sowing of the local photoperiodic variety of mil sanio is spread out during the months of June and July (Ndiaye et al., 2019; Bamba et al., 2019).

3. Materials and methods

Quantifying the impact of dry and wet spells is a multi-step process (Ajetomobi, 2016; Vogel et al., 2019). The main steps include the identification of the study areas, the collection of input data and the definition of a strategy for assessing the contribution of fine rainfall season indicators to yield forecasting. In this study, the model input data include dry and wet spell indicators calculated from In Situ precipitation observations of Senegal's National Meteorology called ANACIM (Fall et al., 2021). In addition, the following indicators provided by the JRC-EU ASAP system were used: a remote sensing biomass proxy (NDVI-METOP), a water satisfaction index (WSI), the 3-month standardized precipitation index derived from CHIRPS rainfall estimates (SPI-3) and ECMWF global radiation (RG) cumulated from June. The ASAP indicators, dry/wet spells and yield data provided by DAPSA were fed into the CST database.

3.1. Rain gauges data and Kriging

Daily rain gauge data used in this study are provided by the national meteorological service of Senegal (ANACIM) for the 1991–2010 period (see Fig. 1). Two levels of quality control were performed. A manual check for anomalous records was carried out, then, further checks were performed including verification of station locations, identification of repeated data, identification of outliers. Finally, comparative tests using neighbouring stations and investigation of suspicious zero values or missing rainfall data was performed (Maidment et al., 2013). These steps are essential to ensure that the model input data is sufficiently clean.

Daily rainfall data from stations were converted to rainfall on grids of $0.25^{\circ} \times 0.25^{\circ}$ spatial resolution using block kriging (BK), a method recommended to transform point-wise rainfall into areal rainfall. BK uses a moving neighborhood or block of given dimensions to estimate the average rainfall value over a surface (Lloyd and Atkinson, 2001; Maidment et al., 2013; Isaaks and Srivaski, 2020). The main benefit of the spatial interpolation of rainfall data is the reduction of the uncertainties and of the sensitivity associated with the point value of a variable rainfall field (Lloyd and Atkinson, 2001; Maidment et al., 2013). It is also the most robust way to estimate a spatial mean value of precipitation over a region.

3.2. CGMS statistics tool (CST) and models

The Crop Growth Monitoring System statistical tool (CST) has been developed by the MARS (Monitoring Agriculture with Remote Sensing) project of the JRC-EU (Kerdiles et al., 2017) to relate crop yield indicators derived from a gridded crop model (e.g. simulated biomass during the crop season or final yield), weather or remote sensing indicators observed during the season (i.e. in advance of harvest) to crop yield statistics at national or sub national level. CST includes data quality checking, time trend analysis of yield statistics to account for technological progress and two models of yield forecasting: (1) multi linear regression analysis which relates crop yield indicators measured during the crop season and final yield; and (2) scenario analysis which looks for the past years that are most similar to the current year according to a set of indicators and combines their yields to make a forecast. CST computes a number of statistics that allow selecting the best model for a given region and time of prediction and therefore to predict yield for the current growing season. In this study we used multiple linear regression analysis to assess the linear relationship between a dependent variable (yield y) and one or more independent variable(s) (the predictor(s) X1, X2...) through the following Eq. 1:

$$y = \beta_0 + \beta_1 \chi_1 + \beta_2 \chi_2 + \dots + \beta_n \chi_n + \varepsilon \tag{1}$$

In this equation $\beta_0...\beta_n$ are the regression coefficients to be estimated through the ordinary least square method which minimizes the difference between the observed and estimated yield values. ε is the random error assumed to follow a normal distribution of mean 0 and variance σ^2 . Errors for different years are assumed to be independent. CST tests various models, using from 1 to 4 predictors (by default) and produces standard statistics and graphs to assess the quality of these models. It also allows controlling multicollinearity between predictors as it reduces the precision of the estimate coefficients. Its strength resides in its capacity to test many models rapidly (e.g. the same model based on one indicator or a set of indicators on several regions and for all the dekads of the growing season; Kerdiles et al., 2017; Goedhart et al., 2017). The standard analysis workflow with CST is the following: Once the database of yield and indicator data has been checked for possible errors, the analyst checks the existence of a so-called 'time trend' in the yield time series (by default CST tests for linear and quadratic time trends at a significance level of 2.5%). A positive time trend is often due to technological progress i.e. improved seeds, fertilization, agricultural practices (e.g. irrigation) and CST assumes that yield variations around this trend – when present – are due to weather. The next step of the analysis consists in testing the correlation between the indicators taken one by one or together, without and with time trend (if present).

We finally tested several models in three steps: (1) 12 regions \times 15 dekads (June to October) \times 50 combinations of dry and wet sequence indicators (2) 12 regions \times 15 dekads (June to October) \times 25 combinations of remote sensing indicators. (3) 12 regions \times 15 dekads (June to October) \times 25 combinations of dry/wet sequences and remote sensing indicators. To simplify the modelling protocol we will use the term "Best DWS" (Best Dry and Wet Spells) to refer to the best combinations of dry and wet sequences. Best RS (Best

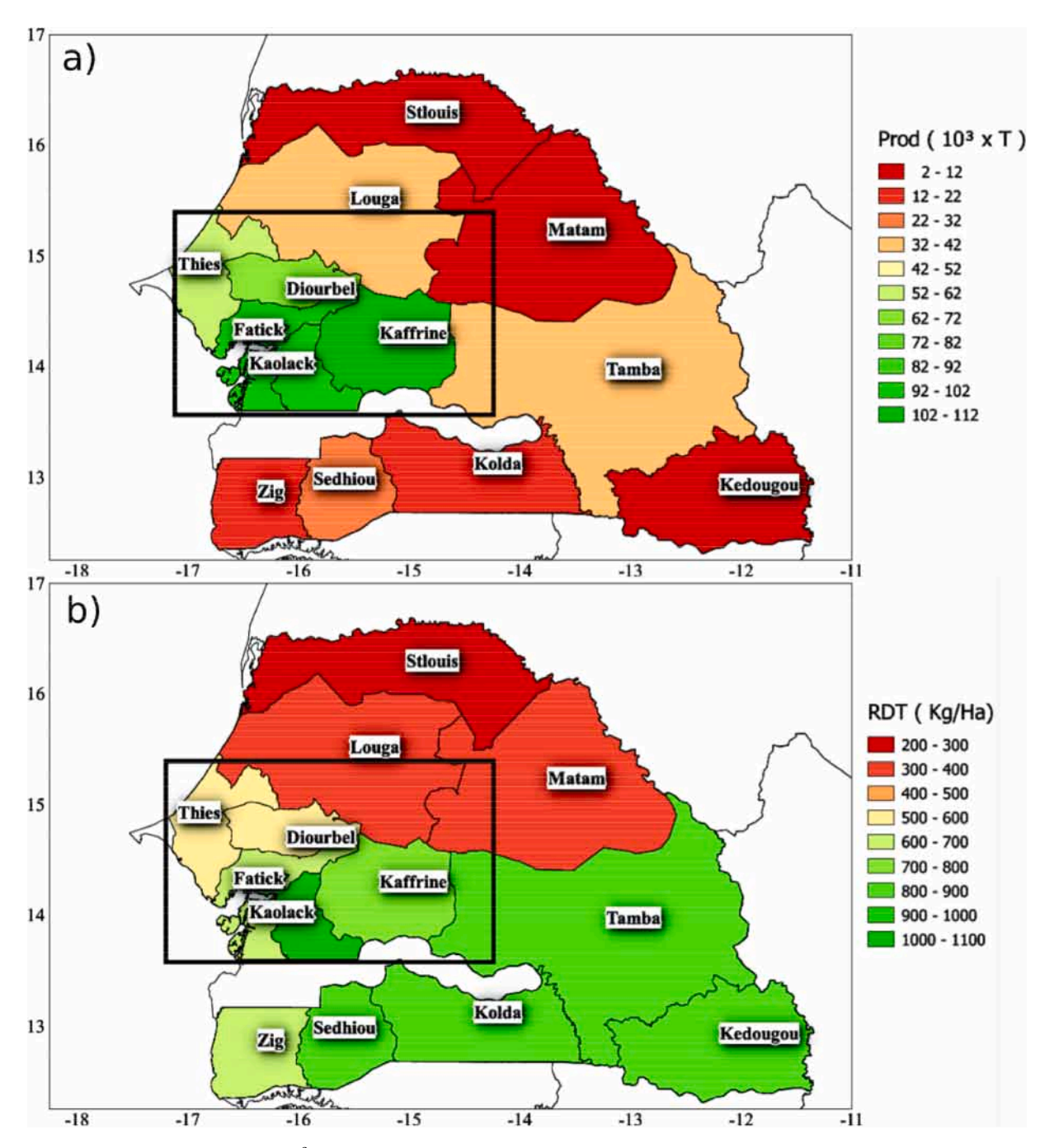


Fig. 2. Average production of millet ($10^3 \times Tonnes$) per region of Senegal provided by DAPSA from 1991 to 2010 (a). Average of millet yield by region computed as the ratio of production and area cultivated from 1991 to 2010 (b). Labels represent the names of the 13 regions of Senegal where agricultural data in millet are available. The square in central western of Senegal illustrates the location of the groundnut basin (area of high density of raingauges).

Remote Sensing) will refer to the best combinations of remote sensing indicators. Finally, we will use the term "Best DWS-RS" (Best Dry and Wet Spells-Remote Sensing) for the best combinations of remote sensing indicators and dry and wet sequences.

In this study, we ranked models according to the root mean square error of prediction (RMSEP), but also looked at the coefficient of determination (R^2) . Indeed, R^2 , which gives the percentage of variance explained by the model is an indicator of the goodness of fit of the model (of its calibration) while RMSEP gives an indication of the quality of the model in prediction conditions. RMSEP is also called the leave one out residual or PRESS statistic.

Table 1
Four remote sensing indicators used in this study downloaded from the Anomaly Hotspots of Agricultural Production (ASAP), the global early warning system of the JRC-EU.

remote sensing Indices	Definitions	Period
WSI	Water Satisfaction Index	1991–2010
SPI-3	Standardized Precipitation Index 3 month	1991-2010
RG	Global Radiation	1991-2010
NDVI	Normalized Difference Vegetation Index from METOP/AVHHR	1991–2010

$$R^{2} = \left(\frac{\sum_{i=1}^{n} (O_{i} - \overline{O}) (P_{i} - \overline{P})}{\sqrt{\sum_{i=1}^{n} (O_{i} - \overline{O})^{2}} \sqrt{\sum_{i=1}^{n} (P_{i} - \overline{P})^{2}}}\right)^{2}$$

$$(2)$$

$$RMSEP = \sqrt{\frac{1}{n} \sum_{i=1}^{n} (P_i - O_i)^2}$$
 (3)

where P_i and O_i are the predicted and observed values for each year i, respectively; \overline{O} and \overline{P} express the mean of observed and predicted values, respectively; n is the number of samples (years). Note that in Eq. 3 the predicted yield for any year is obtained by removing this year from the data used to fit the model; this is to be in prediction conditions such as when we predict the yield of the current year using past data. Predictions become increasingly accurate as RMSEP approaches 0 and \mathbb{R}^2 approaches 1.

3.3. Crop datasets

Official agricultural statistics of millet used in this study were provided by Direction de l'Analyse, de la Prevision et des Statistiques Agricoles of Senegal (DAPSA) (Diagne and Cabral, 2017; Jacques and Defourny, 2019). Note that Senegal's statistical capacity is good compared to the African average; according to the statistical capacity score computed by the World Bank, Senegal ranked second among all sub-Saharan Africa countries in 2017 (datatopics.worldbank.org/statisticalcapacity). Crop yields are based on a two-stage stratified sample of 6300 agricultural households in accordance with an harmonized approach intended to be applied similarly in all countries of the CILSS (Comité inter-États de lutte contre la sécheresse au Sahel). First, between 18 and 30 census districts (CDs) are randomly drawn in each of Senegal's 42 departments (Dakar is largely urban and is not included). Data collection is divided into two phases. During Phase 1, which starts at the end of August, the crop area is estimated. The crop type and location of all fields of each sampled household are recorded. Phase 2 begins in October at the end of the growing season. At that time, the yield is estimated by averaging measurements taken on 60 plots for each crop and department in a sample of the monitored fields. Both phases last 30 days which means that the crop areas are known in September and the yields in November. Spatial distribution of production and yield in Senegal is shown in Fig. 2.

3.4. Remote sensing indicators

For this study, in addition to the dry/wet spells derived from 1991 to 2010 gauge data, we selected four indicators, namely WSI, SPI-3, RG and NDVI extracted at a dekadal (10-day) timestep for each region of Senegal over cropland areas and for the same years (Table 1). WSI and SPI-3 were downloaded from the ASAP website (https://mars.jrc.ec.europa.eu/asap/download.php), while RG was extracted from the JRC repository using SPIRITS (Eerens et al., 2014) and the ASAP cropland mask (Perez Hoyos et al., 2017); as ASAP MODIS NDVI data start only at the end of 2001, we had to resort to the METOP NDVI data from FAO website (http://www.fao.org/giews/earthobservation).

The Water Satisfaction Index (WSI) is an indicator of water availability for crops computed on a dekadal timestep during the growing season since 1991 in ASAP. It is based on the FAO crop specific soil water balance (Frere and Popov, 1986) and uses CHIRPS rainfall (Funk et al., 2015) and ECMWF ERA Interim Penman Monteith evapotranspiration as well as ASAP cropland mask and a generic crop NDVI-based phenology (Rembold et al., 2018). The WSI ranges from 0 (when actual evapotranspiration of crop is nill for all dekads since the start of season due to lack of water) to 100 (the crop water requirements have been fully satisfied since the start of season) (Oosterom et al., 1996; Nieuwenhuis et al., 2006).

The normalized difference vegetation index (NDVI) is a popular green vegetation biomass proxy computed from the visible and near infrared bands of the METOP/AVHRR sensor. NDVI values theoretically range from -1 to +1, with values below roughly 0.2 corresponding to covers other than green vegetation, such as snow, water, clouds or bare soil. Generally, photosynthetically active vegetation has NDVI values between 0.2 and 0.9, with the highest values corresponding to the densest canopies (Wang et al., 2001; Chen et al., 2004).

The standardized precipitation index (SPI) is an indicator of meteorological drought that describes the extent to which cumulative precipitation for a specific time period (e.g. 1, 3, 6 months) departs from the average state, in a similar way as a Z-score (McKee, 1993). Since SPI is standardized, an index of 0 indicates the median precipitation amount for the accumulation period (in our case 3 months),

Table 2Definition of six dry and wet spell indicators used in this study from 1991 to 2010 computed with ANACIM daily raingauges.

Dry Spells Indices	Definitions
DSC20	20 days with less than 20 mm of rainfall
DSs	1-3 consecutive dry days
DSxl	consecutive dry days exceding 15 days
Wet Spells Indices	Definitions
WS1 99 th P	1 day with rainfall $> 99^{th}p$ of daily rainfall
WSM 99 th P	2 day or more with rainfall $> 99^{th}p$ of daily rainfall
WSC5 99 th P	5-d precip. $> 99^{th}$ p of 5-day cumulative rainfall

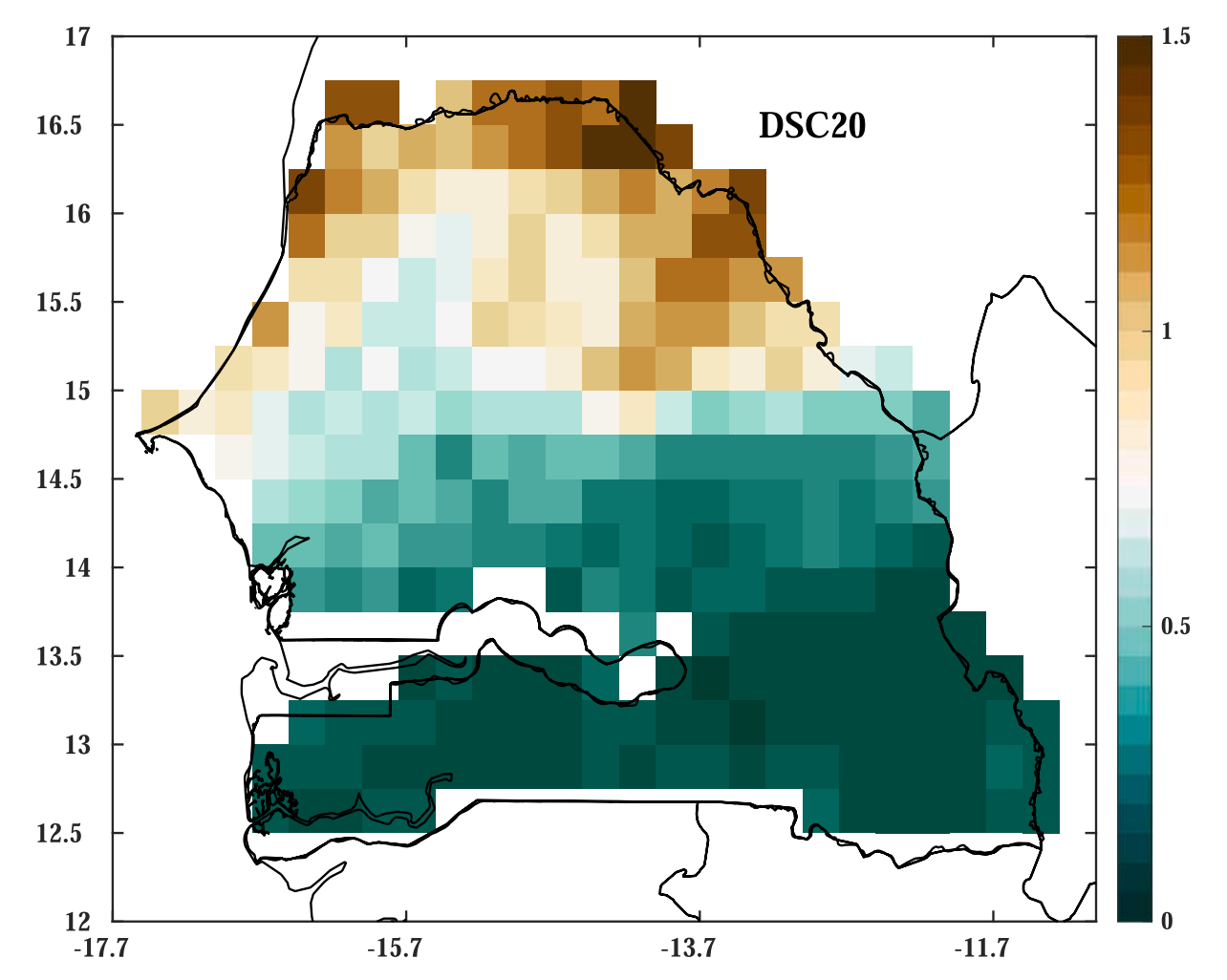
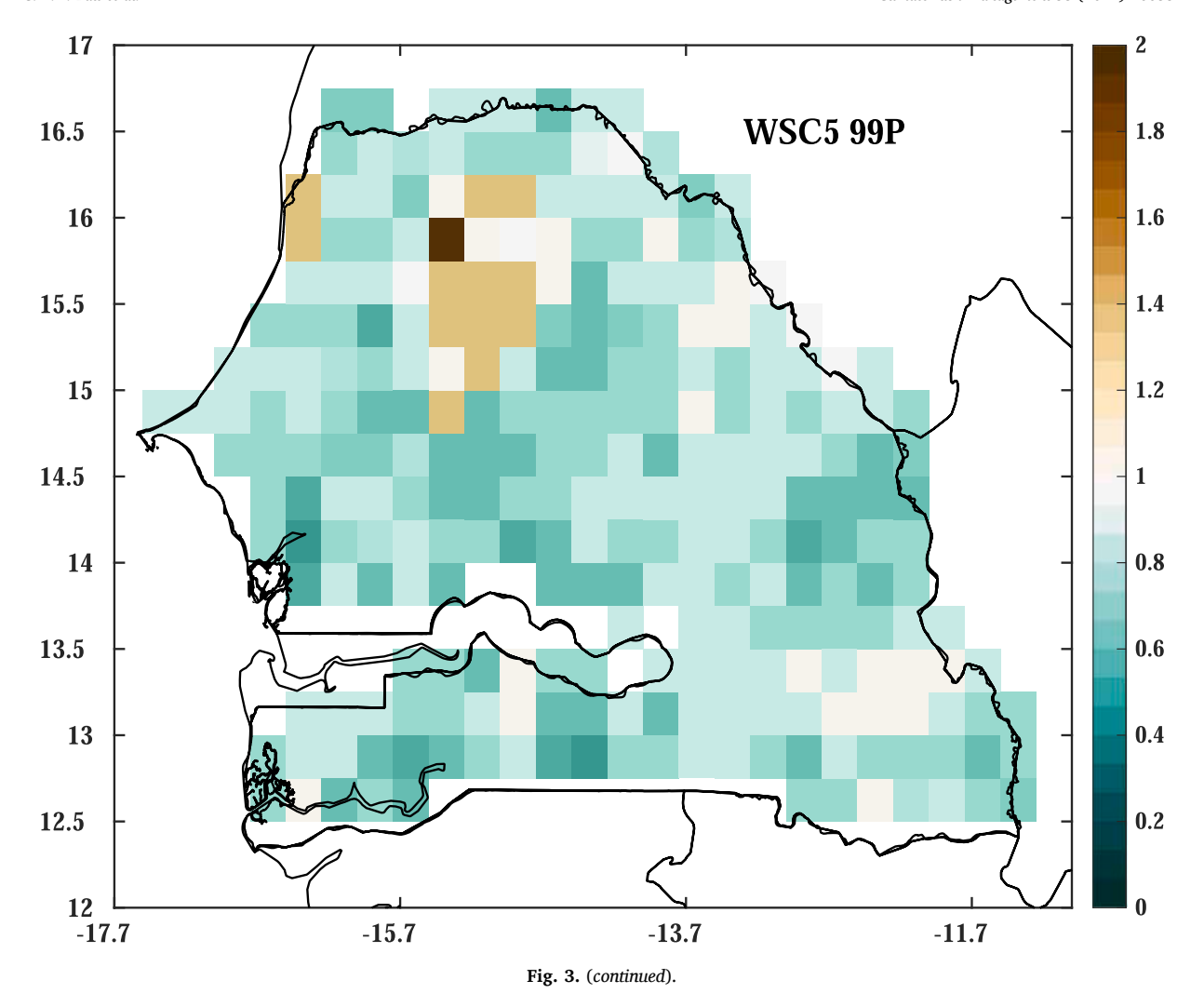


Fig. 3. Spatial variability of six dry and wet spells indicators used in this study. Block kriging (BK) data is used to compute these events during the rainy season (JJASO) for 1991–2010 period.

while dry conditions are indicated by negative values (i.e., below -1.96 for extremely dry with a probability of occurrence below 2.5%) and wet conditions are indicated by positive values (i.e., above 1.96 for extremely wet) (Kumar et al., 2009; Lavaysse et al., 2018).

SPI-3 months was derived from CHIRPS rainfall estimates and in ASAP the times series starts from 1991. Global radiation (RG), which expresses the daily sum of incoming solar radiation that reaches the earth's surface, is also used as a "remote sensing" indicator for this study as it is a driver for photosynthesis and plant growth. RG is mainly composed of wavelengths ranging from 0.3 to $3\mu m$ and approximately half of the incoming radiation with wavelengths between 0.4 and $0.7\mu m$ is used by plants for photosynthesis. In ASAP,



global radiation is derived from ECMWF ERA Interim model data since 1991 and is used in the calculation of Penman–Monteith evapotranspiration.

3.5. Dry and wet spells

Six dry and wet spell indicators were selected based on their duration and intensity from those defined by Fall et al. (2021). For the dry spells, we selected different durations to test different rainfall deficit periods, assuming that the longer the dry spell, the higher their expected impact on crop growth. The three dry spell indicators selected are Dry Spell short duration (DSs, i.e. from 1 to 3 days with less than 1 mm/day), Dry Spell extreme long duration (DSxl, i.e. at least 15 days with less than 1 mm/day) and Dry Spell Cumulative over 20 days (DSC20, 20 days with less than 20 mm) (Table 2).. The three wet spell indicators selected are Wet Spell one day (WS1) to capture daily intense rainfall events, Wet Spell Medium duration i.e. equal or longer than two days (WSM) and Wet Spell Cumulative of 5 days (WSC5) to capture the most intense 5-day cumulative rainfal (Table 2). Note that the 99th percentile of daily precipitation over the 1991–2010 period is used as the threshold for WS1 and WSM, whereas the 99th percentile of the 5-day period is the threshold used for WSC5. Overall, these dry and wet spells are closely related to the intraseasonal variability of the WAM (Dieng et al., 2008; Froidurot and Diedhiou, 2017). Indeed, the establishment of the WAM is characterized by a succession of active and inactive phases, during which rains intensify (wet spell) and weaken (dry spell). The duration categories of wet spells are chosen to correspond to the different synoptic systems driving rainfall in West Africa. The WS1, WSM, WSC5 can be associated with the so-called '3-5 days' African Easterly Waves (AEWs) and the '6-9 days' AEWs (Diedhiou et al., 1998; Lavaysse et al., 2006; Wu et al., 2013). These AEWs are synoptic disturbances known to influence mesoscale convective systems over West Africa. The 20 days duration used to define DSC20 is another variability mode of the African monsoon rainfall that may result from regional coupled land-atmosphere interactions (e.g. Grodsky and Carton, 2001; Mounier and Janicot, 2004.

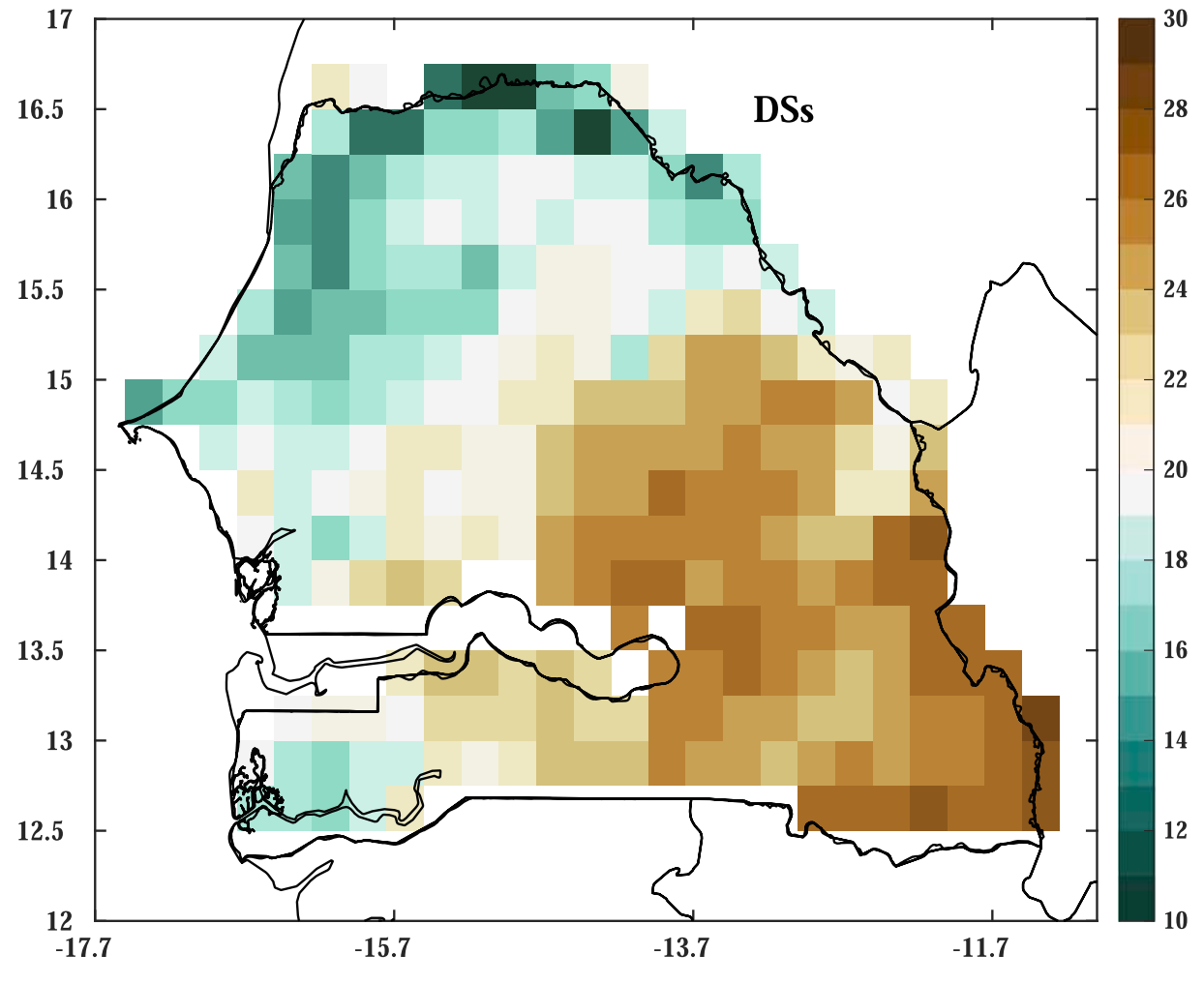


Fig. 3. (continued).

4. Results

4.1. Spatial variability and seasonality of dry and wet spells

The wet and dry spells present important temporal and spatial variabilities. As illustrated in Fig. 3 dry spells show a strong south-north gradient with a stronger occurrence in the north except for DSs. The strong prevalence of DSs in the South is explained by the higher seasonal rainfall, the number of 1–3 day periods without rain increasing with the number of rainy days between DSs by construction of DSs. Conversely, no spatial gradient appears for wet spells. This is due to the definition of WS which is based on the Peak over threshold (POT) method of quantiles, which eliminates the spatial variability of rainfall.

Given the potential sensitivity of crops to the timing of dry and wet spells (Troy et al., 2015), it is interesting to look at the seasonal distribution of DS and WS. The long duration dry spells (DSC20 and DSxl) exhibit fairly similar seasonal cycle with high frequency at the start and end of the season, which makes them effective indicators of false starts and early cessations of the rainy season (Fig. 4). Conversely, DSs display a seasonal cycle close to the daily rainfall, suggesting that they are an indicator of rainy days.

Regarding the wet spells, all of them show the same seasonal cycle with a high occurrence during the peak of the WAM (August–September), when intense organised systems are more frequent. However, there are some differences in the timing within the season for these extreme events. Indeed, isolated extreme wet days (WS1) show a strong spread throughout the season and can even occur at the beginning and end of the season although the probability remains very low (2%) at these times of the season. In contrast for WSC5 and WSM, which are concentrated between July and September, the spread is more narrow as these events are less frequent. This timing can make these extreme events harmful to crops. Indeed, excessive rainfall may result in lodging and pathogen development and, at harvest, may make field operations impossible (Berry et al., 2004, 2011).

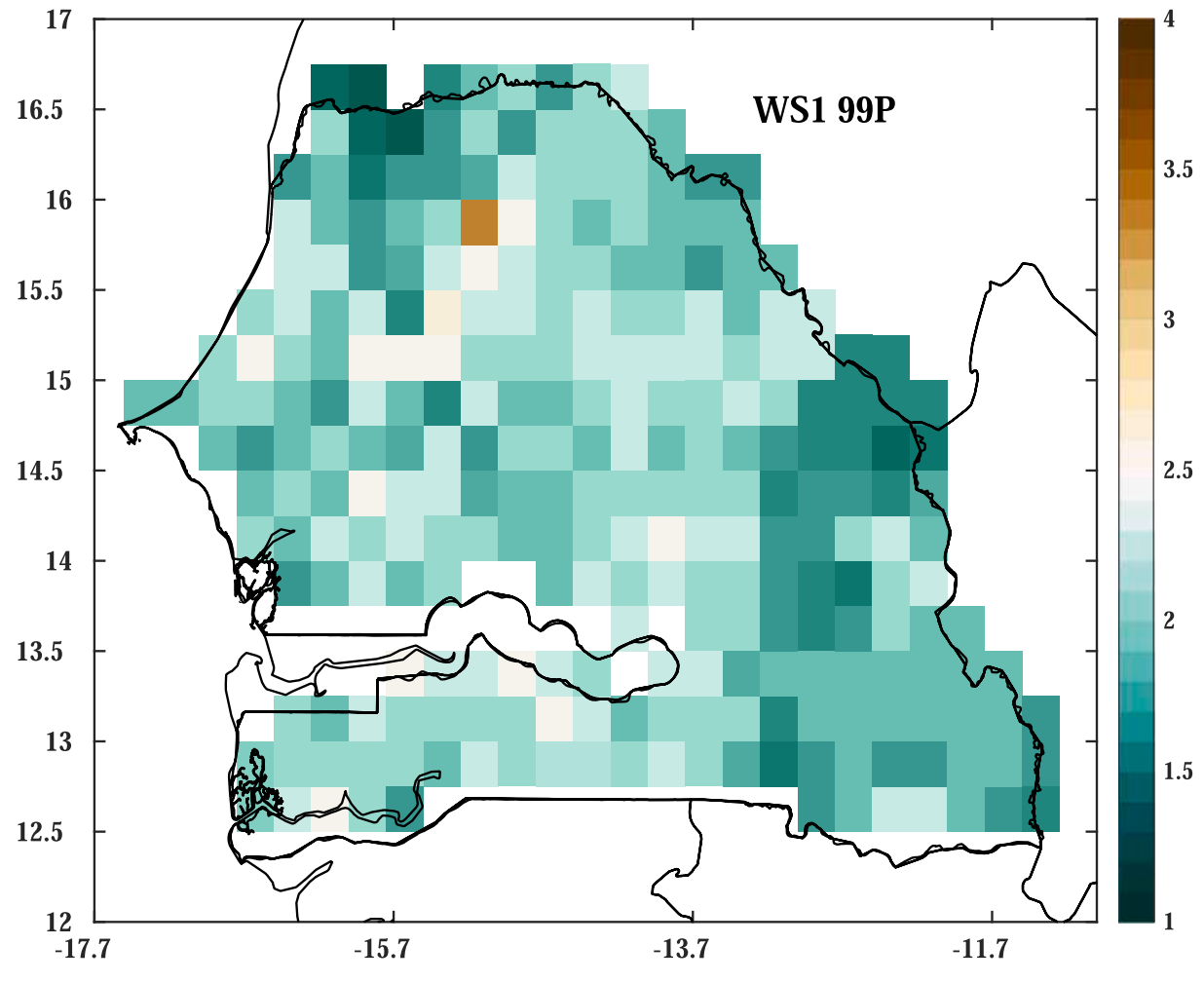


Fig. 3. (continued).

4.2. Spatio-temporal variability of remote sensing indicators

A clear north-south gradient is observed for the average NDVI and cumulated RG over the rainy season (Fig. 5). NDVI generally decreases from south to north and tends to be mainly a function of latitude, due to the relation between green biomass and rainfall (Fig. 1 Li et al., 2004). This strong relationship between rainfall and NDVI is largely explained by the seasonal migration of the tropical rain belt. Indeed, its arrival in the Sahelian zone indicates the beginning of the rainy season and the end of a hydric stress of more than seven months from November to May (Nicholson, 2013). Cumulated seasonal RG decreases from north to south, reflecting the higher rainfall and cloud cover in the south with respect to the north. The interannual evolution allows comparing the average seasonal behaviour of three of the remote sensing indicators and of the rainfall index derived from gauge data (Fig. 6). Some disagreements between the rainfall index and the three remote sensing indicators can be observed. For instance in 2000 NDVI, SPI3 and WSI show a decrease with respect to 1999 and 2001 while the rainfall index has the opposite behaviour. In 1991, it is NDVI that disagrees with SPI3 and WSI. In other years (e.g. 2001, 2002, 2008), we see a fairly good agreement between all indicators. For the intense drought of 2002 (Sagna et al., 2015), WSI recorded its lowest value 40%, NDVI reached its second lowest value after 1991 and, SPI-3 recorded its most negative deviation over the whole period, with a value of -2.5 corresponding to less than the 1% driest years (McKee, 1993). The example of the 2002 drought demonstrates that NDVI, WSI and SPI-3 capture well extreme dry events and their impacts. RG recorded its highest value in 2002 as cloud cover was reduced and rainfall was low. These results extend those of Nicholson et al. (1998). Nicholson et al. (1990) in East Africa, who found that the spatial patterns of the NDVIs each year closely reflect the average annual precipitation.

4.3. Model performance

The multiple linear regression (MLR) model of the CST tool is used to assess the contribution of the indicators listed in Table 1 and 2

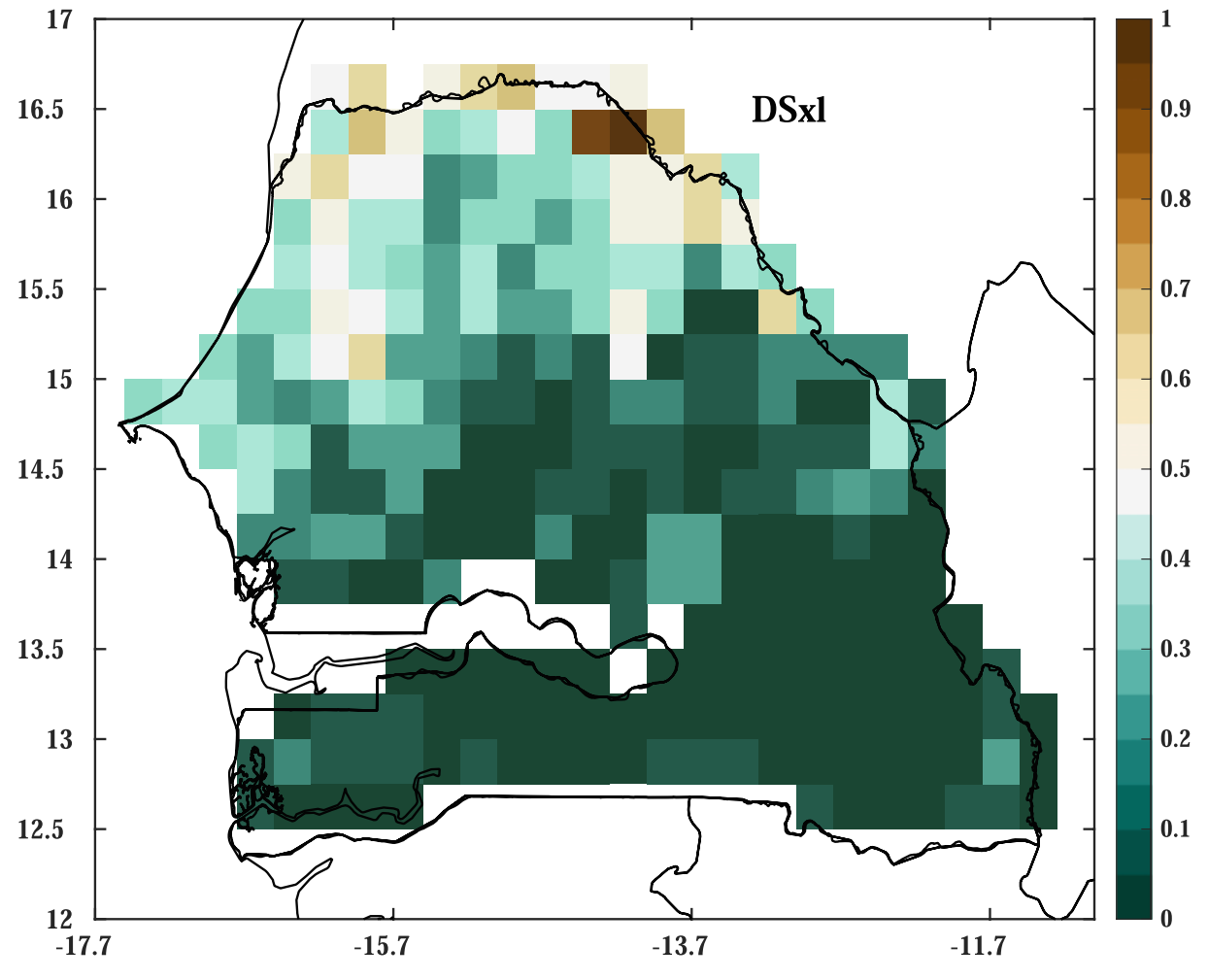
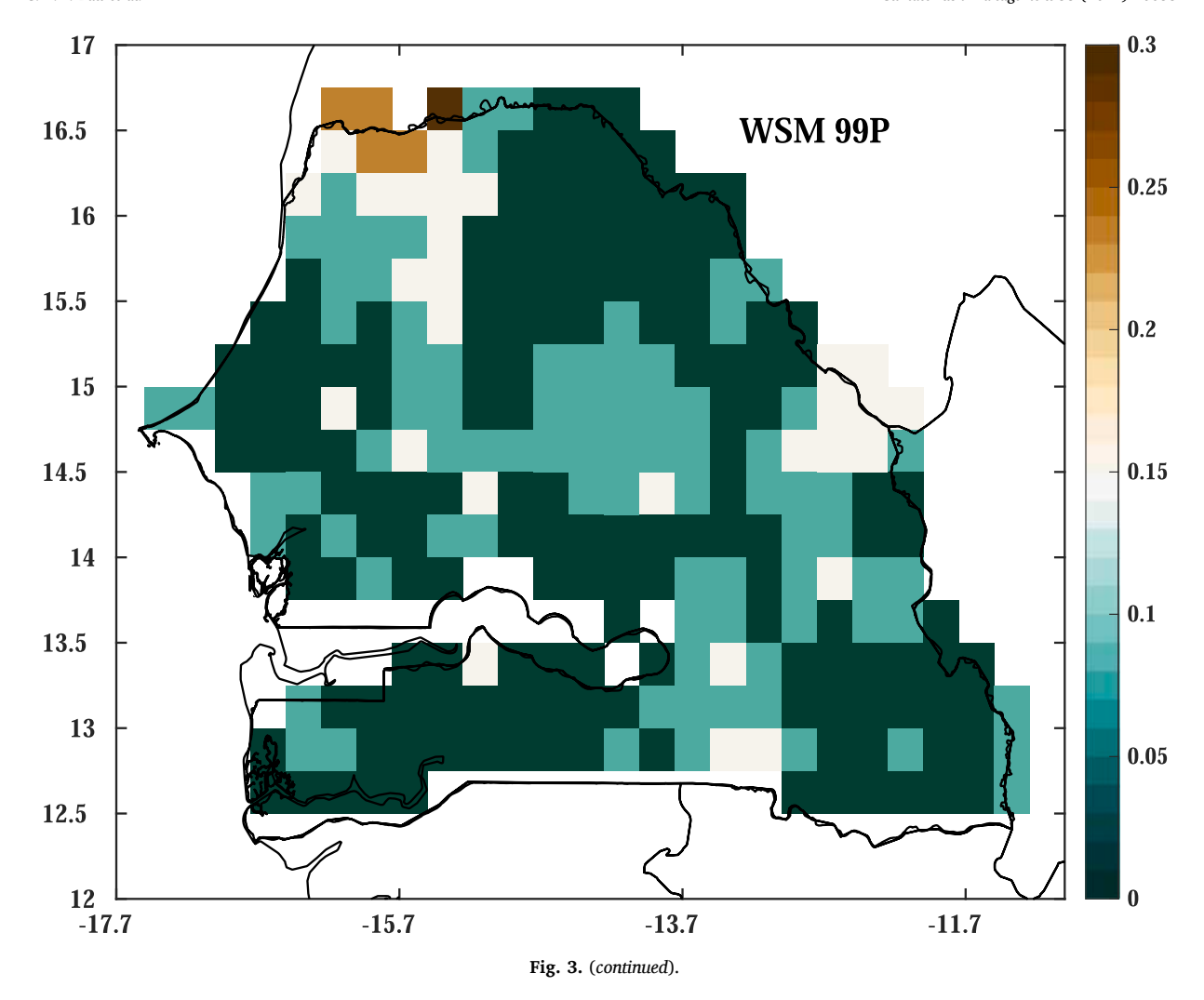


Fig. 3. (continued).

for forecasting millet yields in Senegal. Two parameters computed for each tested model are analysed, namely R², which measures the proportion of variance in yield data explained by the predictors, i.e. the goodness of fit of the model based on all available years, and RMSEP, the root mean square error of prediction. Using CST standard mode, none of the 12 regions of Senegal showed a significant time trend (at a 2.5% significance level, not shown) for millet yields over the period 1991-2010, suggesting that yield variations due to technological progress are low or lower than weather induced variations. At a level of 5%, two regions, Matam and Thies, show a significant quadratic trend with lower yields in the years 1997-2004 and slightly higher yields before (i.e. years 1991-1996) and clearly higher yields after, especially around 2008–2010. Since the significance of this trend is not strong (post 2010, these two regions show no significant trend, see Fig. S1 in supplementary material) and the causes for the relatively higher yields of years 1991–1996 are unclear, the time trend of these two regions has been considered irrelevant and we assume that weather was the main responsible for yield variations during the 1991–2010 period. After having tested the time trend, the next step is to identify the regions of the country where the model has statistically significant scores. Fig. 7 shows the best R² of the significant runs of the model for each dekad. These runs are testing the correlations between millet yields and dry/wet spells combined with remote sensing indicators. We observe significant correlations between millet yields and our indicators over several dekads but with a strong spatial and intra-seasonal variability in the R² scores. In only two regions out of twelve, we have either no significant relation (Ziguinchor or Zig, which represents on average 1% of national millet production) or a significant relationship only for one dekad (Sedhiou, 6% of national production). For the remaining 10 regions, we have significant R² mainly from end July to end October. In the five regions of the groundnut basin, namely Fatick (19% of national production), Kaolack (18%), Kaffrine (18%), Djourbel (12%), and Thies (9%), to which could be added Louga (5%) for its southern half, we have strong disparities in the quality of the relationship. Kaffrine and Kaolack recorded their highest scores at the beginning of the season (June and July respectively). Fatick, Diourbel, Thies and Louga show fairly similar trends covering most of the decades. Overall, Thies remains the best region where R² varies between 60 and 80% with a great stability throughout the season. The density of the rain gauges does not explain the good performance of the indicators in Thies since there is an equivalent gauge network in Kaolack and Fatick. The origin of these better relationships is still unclear. They



could be due to a better quality of agricultural data. To confirm this hypothesis, a thorough evaluation of the quality of official statistics should be carried out.

4.4. Prediction quality

The consequences of wet and dry spells depend on their intensities, and timing within the season. Dry spells can generate high impacts especially when combined with high temperatures. Extreme wet spells can damage crops when associated with heavy rainfall (or rarely hail) and potentially cause intense runoff during persisting rainfall generated by high occurrence of MCSs. Nevertheless, mild wet spells may have benefits when the intensities and the persistence are not high. To better understand the impact of the single indicators on crop yields, the sign of the regression coefficients or slopes for individual indicators are illustrated in Fig. 8 with the level of R² scores for each dekad in Thies. Regarding dry spells, as expected, DSxl and DSC20 are negatively correlated with yields from mid June and early July respectively till end October while DSs, which increases with rainfall, is positively correlated with yield from July to mid August, i.e. in the early vegetative growth of the crop. As for wet spells, WSC5 and WS1 are positively correlated with yield as from end of August – early September till end October and the most extreme wet spells (WSM) do not show any significant effect on yield in Thies. This suggests that wet spells are not able to capture the potential damage (flooding, disease) that they may cause to crops. Actually the two years with the highest number of WSC5, 2008 and 2010 (Fig. S11 in supplementary material) are characterized by high yields. In other words, at regional level, the crops benefited from the abundant rainfall provided by the WS and were not impacted negatively by diseases, lodging or floods. According to the test protocol, the six dry and wet period indicators are combined to obtain the "Best DWS" and the four remote sensing indicators are also combined to obtain the "Best RS". For each dekad of the season the best indicator or combination of indicators is highlighted. The performance of the indicators in each dekad of the rainy season is illustrated by the coefficient of determination (R2, Fig. 8the root mean squared error of prediction (RMSEP, Fig. 9c,d).

Firstly for dry and wet spells, Fig. 9a shows two behaviours depending on whether the event is dry or wet. For dry spells (DSC20, DSs, DSxl), prediction is earlier than for wet spells with significant relationships observed in mid June for DSxl and in the first dekad of

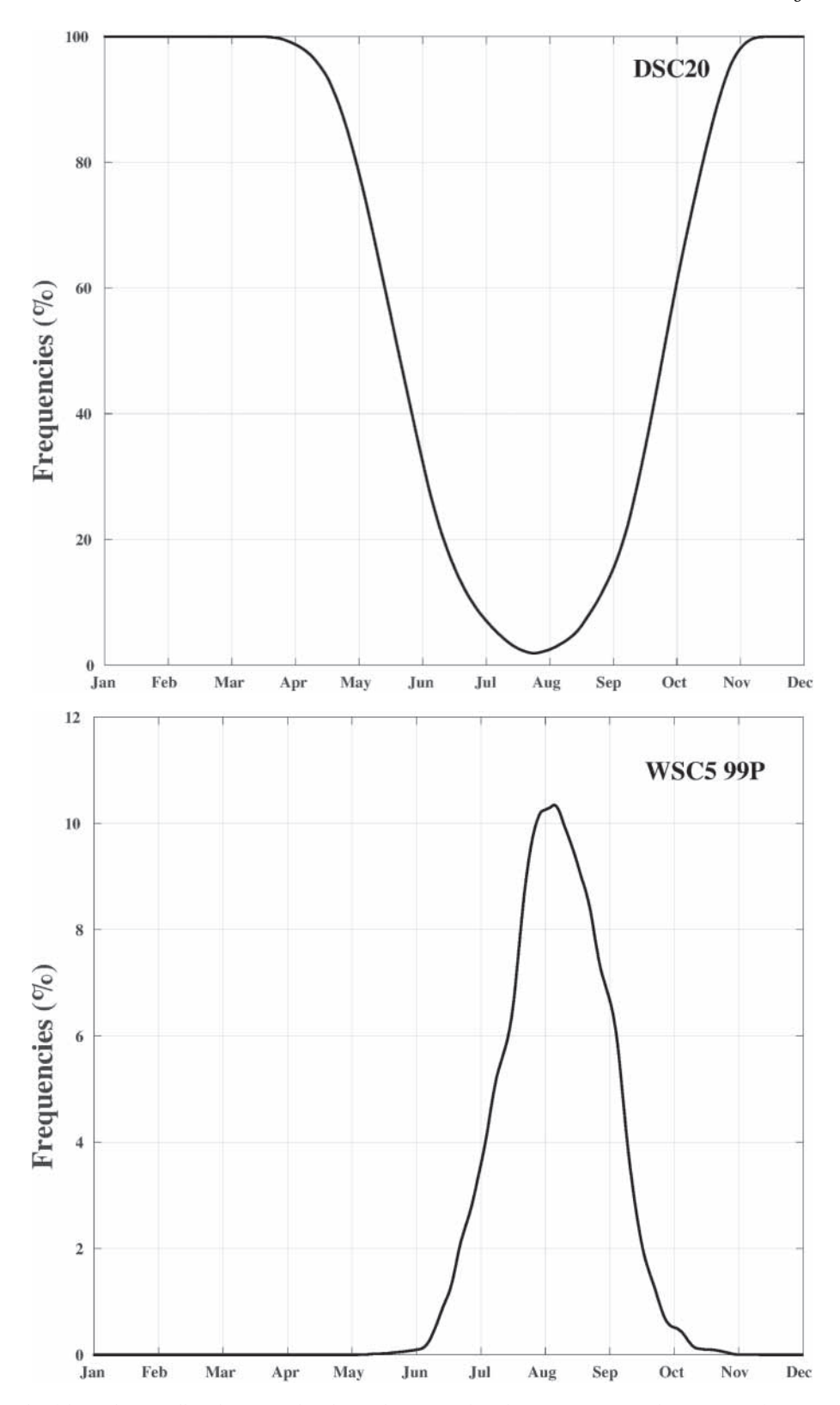


Fig. 4. Annual cycle of dry and wet spells indicatos used in this study computed on the 1991–2010 period. Frequency of occurrence is defined as a ratio of observational days with recorded dry or wet spells.

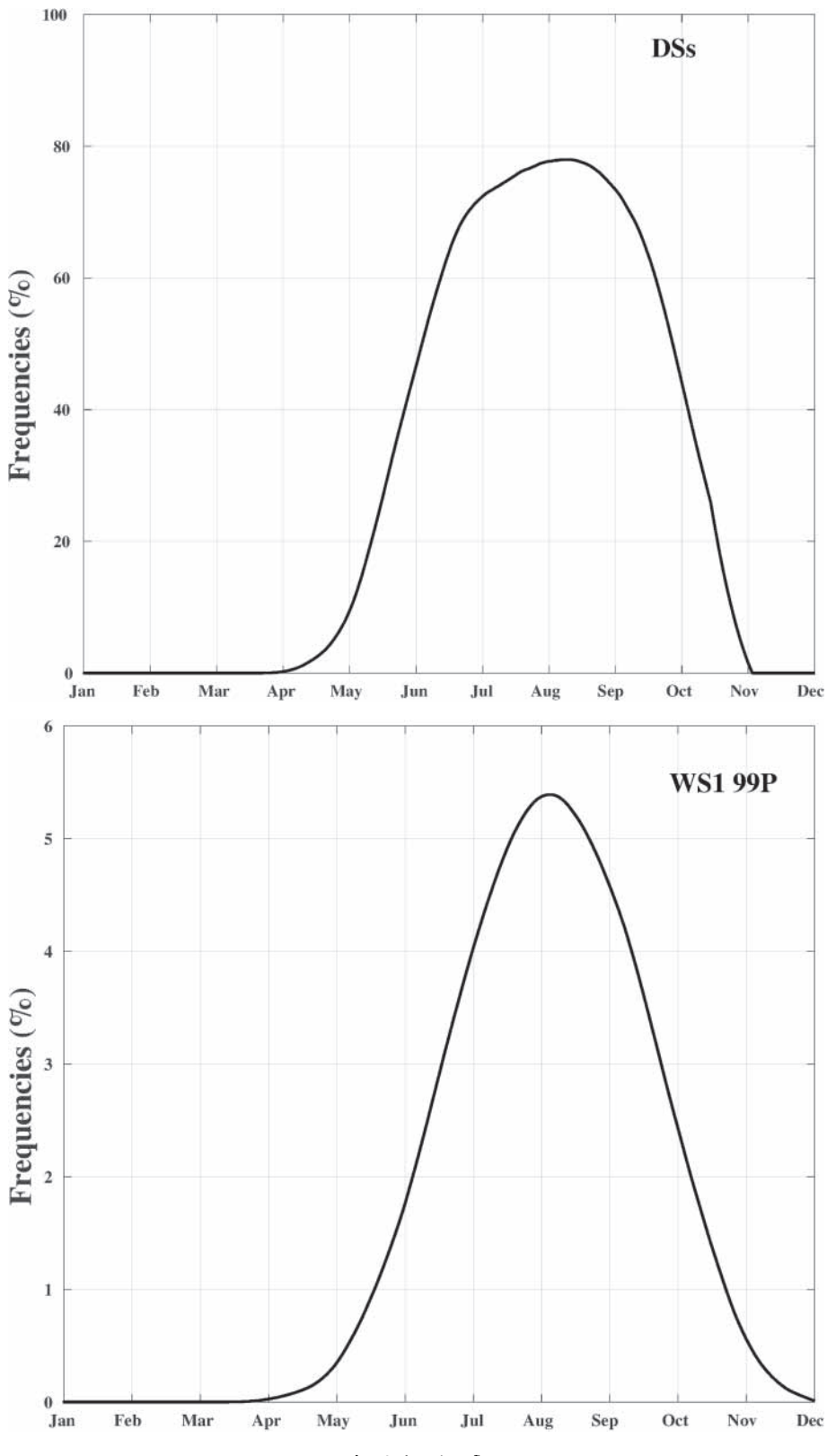


Fig. 4. (continued).

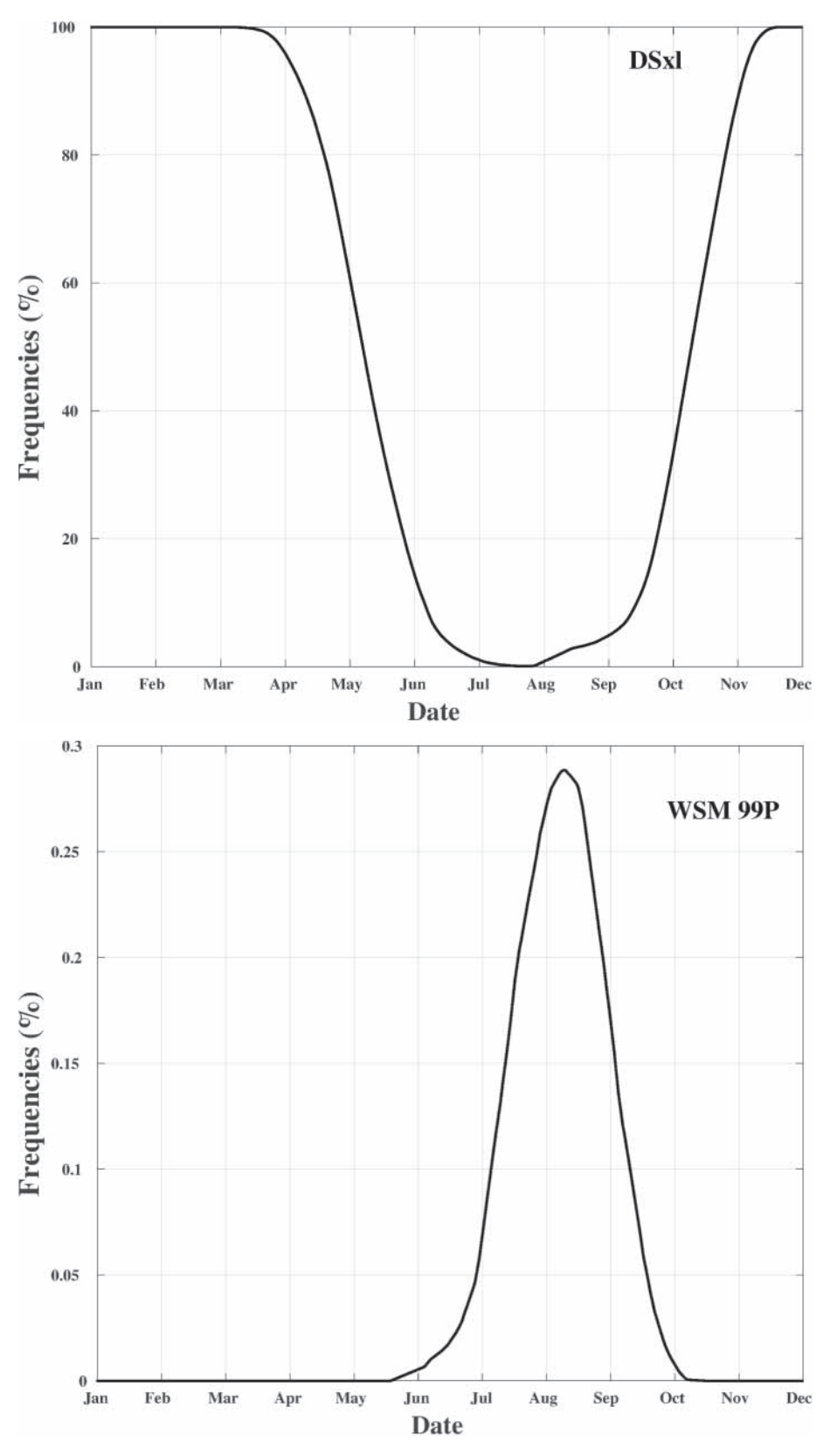


Fig. 4. (continued).

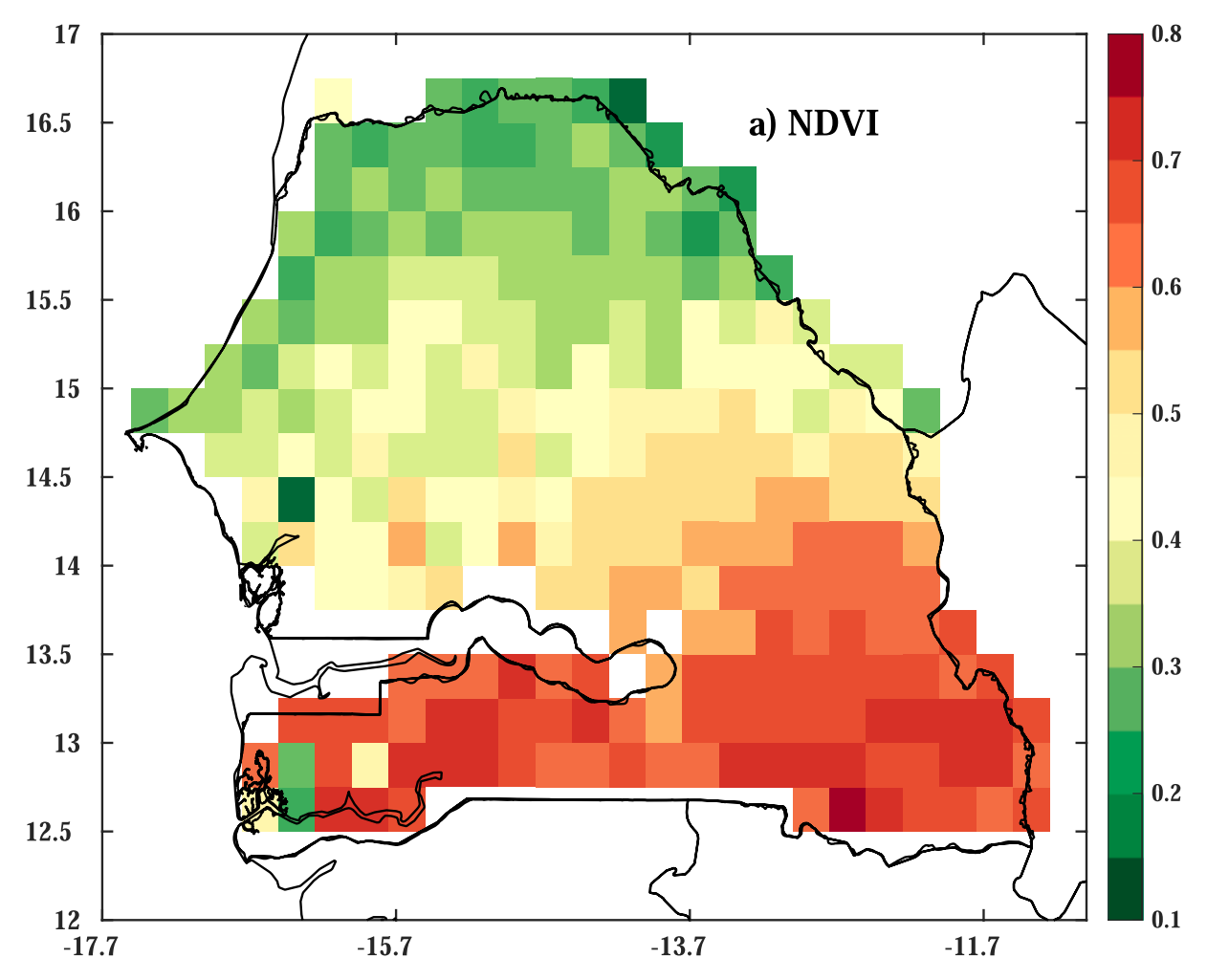


Fig. 5. Spatial variability of the average seasonal index calculated over the 1991–2010 period. Water satisfaction index (WSI), Global Radiation (RG) and Normalized difference vegetation index (NDVI). WSI just captures information on the active pixels of crop mask with 0.25° as common resolution.

July for DSs and DSC20. This performance of dry spells at the beginning of the season could be related to the sensitivity of young plants to prolonged dry spell (USAID 2014). Indeed, recent studies on the rainfall seasonal cycle across Sahelian countries (Le Barbé et al., 2002; Lebel et al., 2003; Sultan et al., 2003) show the existence of two rainfall phases. The first phase corresponds to a progressive onset of rain on West Africa originating from the tropical Atlantic (June – beginning July). For that reason, this phase is considered to be similar to an oceanic regime marked by a high occurrence of dry spells. The second regime is continental and corresponds to the most active phase of the WAM (July to September) with a high occurrence of organized mesoscale systems that give origin to wet spells. This timing of wet spells explains their influence on millet yields from the last dekad of August onwards. Individually DSC20 seems to perform better than WSC5, the best wet spell, and explains up to 50% of the interannual variability in millet yields. The best DWS is a combination of DSC20 DSs and WSC5 over September-early October which reaches an R² of nearly 80% in mid September.

The relationships between millet yield and the remote sensing indicators are shown in Fig. 9b. All indicators appear to be significant with R^2 around 35–40% in mid July, which corresponds to the early vegetative development of the crop (see temporal evolution of NDVI – Fig. S2 in Supplementary Material). R^2 reaches a maximum (around 60%) with NDVI in August, whereas other studies found the best correlation around the time of maximum NDVI, which in Thies occurs in September – early October (e.g. Rembold et al., 2013). WSI and SPI3 depict a plateau of R^2 from mid July till end October. This is possibly due to their stronger temporal autocorrelation, with a maximum R^2 (45–50%) in early September, when panicle initiation starts. The peak for SPI3 corresponds to the rainfall during the period of vegetative development for the crop (June to September). The sign of regression coefficients with millet yield are positives for NDVI, WSI and SPI3. In contrast, RG is negatively correlated with yield, suggesting that RG as a proxy of deep convection is more important than its role in photosynthesis, which is not a limiting factor. This was also mentioned in previous study (Vijayalakshmi et al., 1991; Islam, 1992) for rice in the tropics but a proxy for crop water stress during the whole season (cf. Fig. 8).

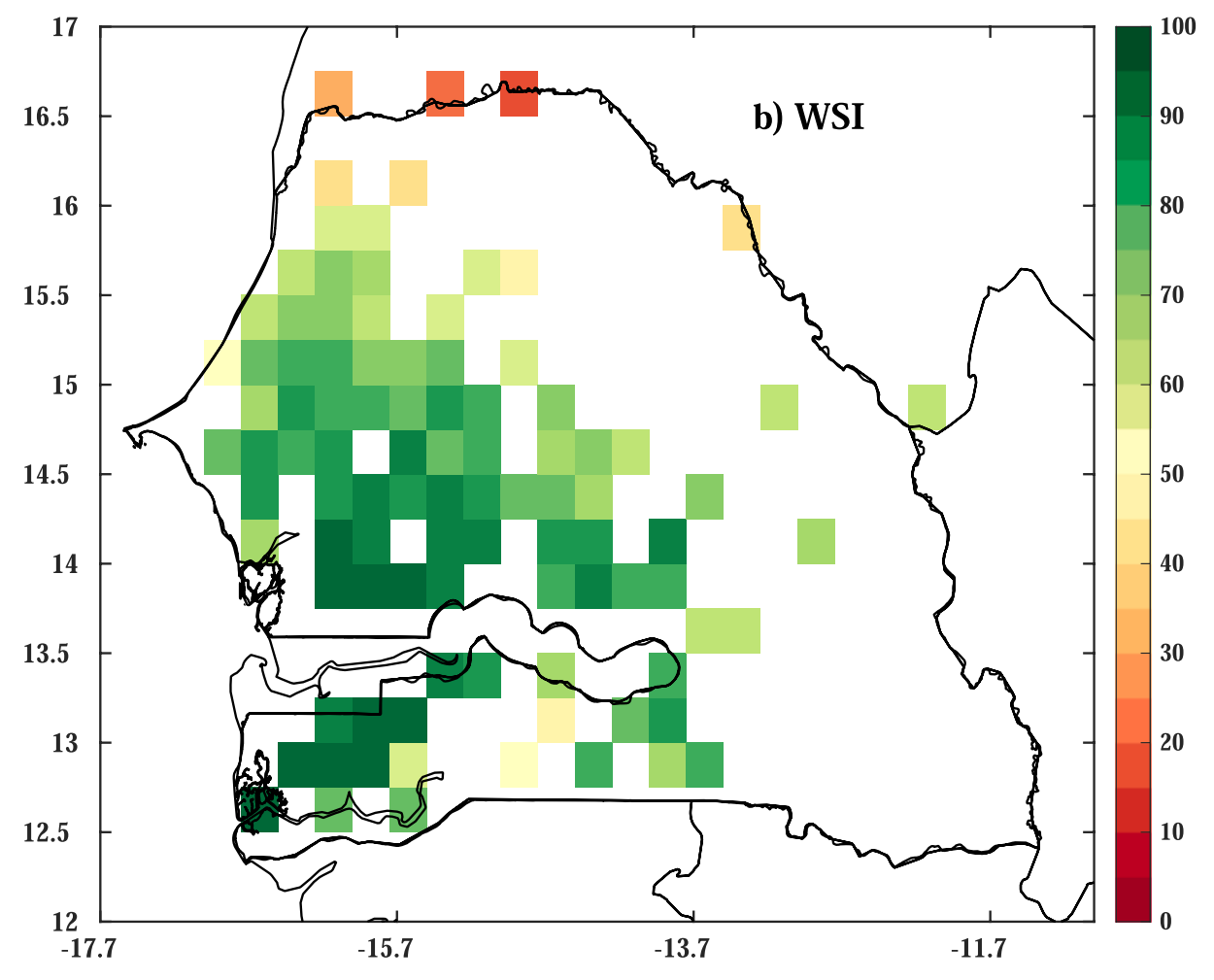


Fig. 5. (continued).

The RMSEP of both wet and dry spell and remote sensing indicators show similar trends to R^2 with a more accurate prediction in August and September for dry and wet spells respectively as illustrated in Fig. 9c,d. We can compare the effectiveness of the dry and wet spell indicators versus remote sensing indicators in predicting yields. The only remote sensing combination that can achieve a RMSEP of 100 kg/ha (i.e. about 20% of the mean yield of 479 kg/ha) is the RG-NDVI combination in the third dekad of August while the best combination of DWS (DSC20-DSs-WSC5) reaches this value one dekad later in early September.

Fig. 10a shows the temporal evolution of R² for the best combination of remote sensing indicators, dry and wet spell indicators and all indicators together. Early in the season from mid June to mid July, DSxl and DSC20 are the best indicators, which suggests an impact of dry spells and false start of the rainy season at crop emergence on final yield. As from the second dekad of July, combinations of indicators outperform individual indicators. DSC20-WSI starts with an R² around 60%. Between the third dekad of July and the first dekad of September, the best combination includes NDVI with two dry spells indicators (DSC20 and DSs) and a wet spell indicator (WSC5) while from mid September to early October the same two dry spell and wet spell indicators perform better. For the last two dekads of October, a combination of DSxl and RG is the best performer. The best predictor which also explains nearly 80% of millet yield variations, is reached on the first two dekads of September by the DCS20-DSs WSC5 combination with and without NDVI. DSC20 is strong drivers of millet yield and are identified in most combinations, especially during the panicle initiation (August-September).

The strong impact of mid-season combinations during the flowering and grain-filling phases is mainly explained by the fact that this is the period when crop water requirements are the highest. For example, a DSC20 that occurs in the context of a water balance deficit has a more negative effect on yields. This pattern is fairly well illustrated by combinations such as DSC20-DSs-WSI, DSC20-NDVI and DSC20-DSs-WSC5-NDVI. It is important to note the surprising performance of RG which is observed in two of the seven best combinations. Indeed, RG does not show high scores when tested alone. And actually the combination DSxl-RG has a significant relation with yield at the end of the season. The other trend highlighted by Fig. 10a is the impact of dry and wet spells on yields in the heart of the monsoon (third dekad of August to first dekad of October). Indeed, the improvement achieved by the integration of remote sensing indicators is almost insignificant as long as dry and wet spells are effective at this time of the season. Fig. 10b) assess the predictive capacity of the combined indicators, for each dekad by the RMSEP. At the beginning of the season the difference between the RMSEP of

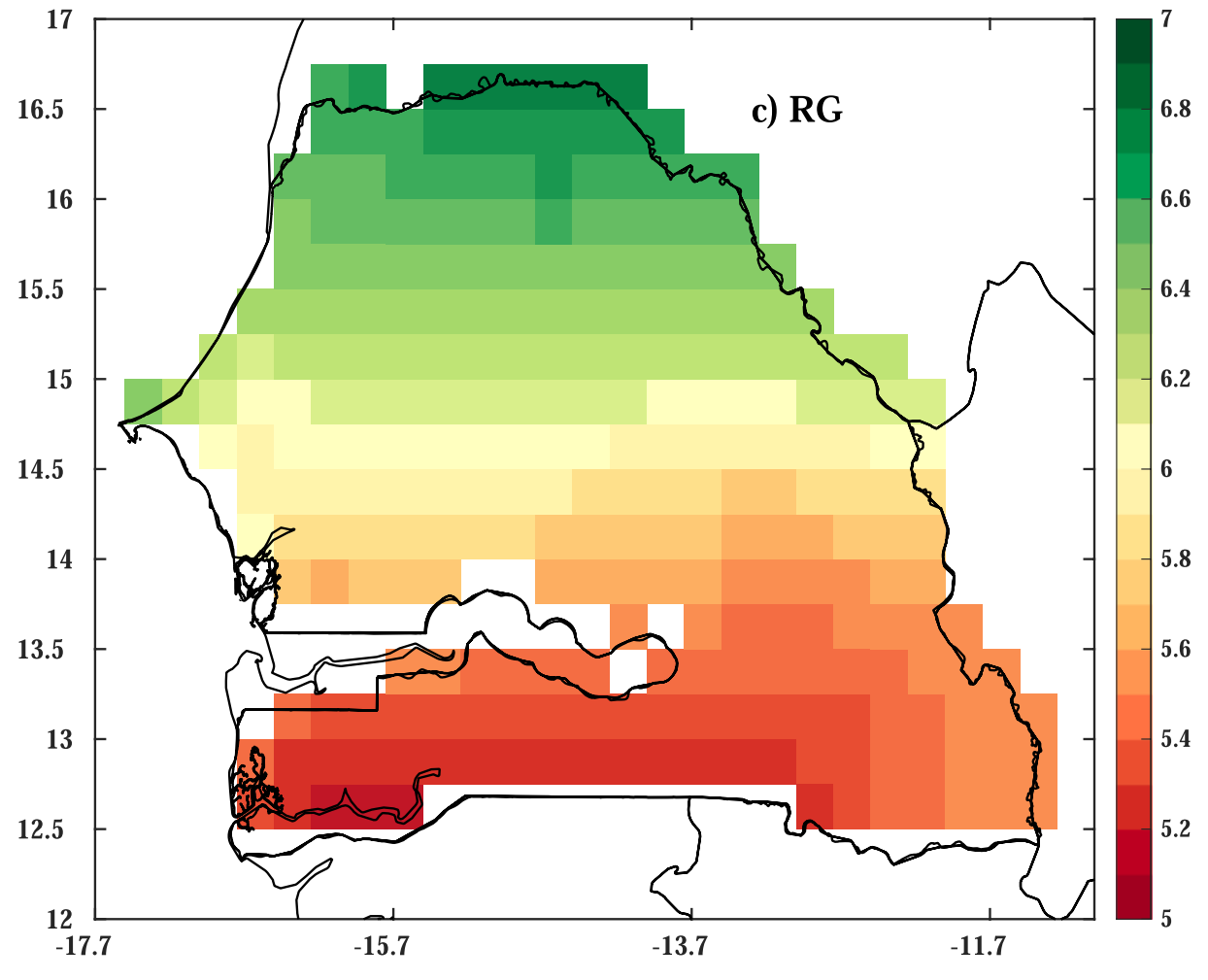


Fig. 5. (continued).

the best RS model and the best DWS model can reach 50 kg/ha (about 10% of the mean yield) before reducing to 10 kg/ha (2% of the mean yield) between the third dekad of August and the first dekad of October. As from September the RS performance decreases with an RMSEP above 120 kg/ha versus 90–100 kg/ha for the DWS. This means a more accurate forecast with dry and wet spells during the peak of the monsoon. These results highlight, once again, that the impact of DS depends on their timing with respect to the crop phenology and condition, which can be monitored with RS indicators.

Fig. 11 shows the best combinations found for the 12 regions of the country at the start of each month between July and October. In July DSC20 appears to be selected in 4 of the 6 regions having a significant relation, mostly in the western half of the country. Apart from this case, no specific indicator appears to be predominant in the three other periods (early August, September and October). The best correlations were obtained for September at the time of flowering with a diversity of combinations of indicators. Wet spells, which mostly occur from July to September, are more significant in September and October. Although the importance of the other characteristics should not be overlooked, multicollinearity may make them appear less important in some regions of the country. The effectiveness of the DSC20 and DSxl indicators is highlighted in the groundnut basin regions in July as well as for the northern regions of the country. However, in the southern part of the country, only SPI3 and NDVI indicators seem to have an impact on millet yields. The dry spell indicators perform worst in the south of the country, due to the definition of dry spells which does not use a threshold based on rainfall quantiles, unlike the wet spell indicators. Finally, we can see the occurrence of RG and WSM in most of the best combinations in the south east of the country in early September. The high occurrence of WSM alone or combined with SPI3 or RG in the best southern combinations can be related to the percentile methodology used to detect extreme wet spells. Indeed, the thresholds obtained in the south allow to identify more intense rainfall compared to the north and the groundnut basin (See Fig. S4 in supplementary material). Therefore, extreme events in the south are more susceptible to negatively impact yields. The R² trends are confirmed by the spatial distribution of the RMSEP.

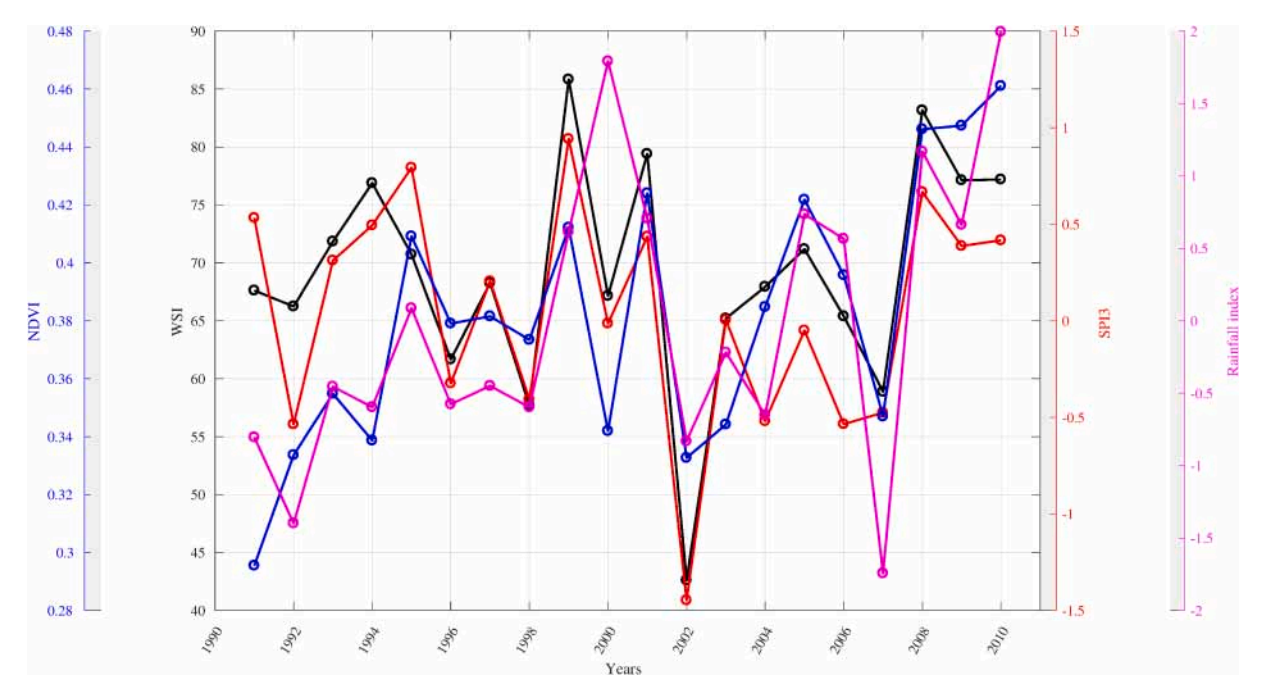


Fig. 6. Inter-annual variability of Water satisfaction index (WSI), Standardized precipitation index 3-months (SPI-3) and Normalized difference vegetation index (NDVI) averaged over the (JJASO) season. The magenta line illustrates the Lamb index, i.e the Z score of the rainfall cumulated from June to October (see Abbam et al., 2018).

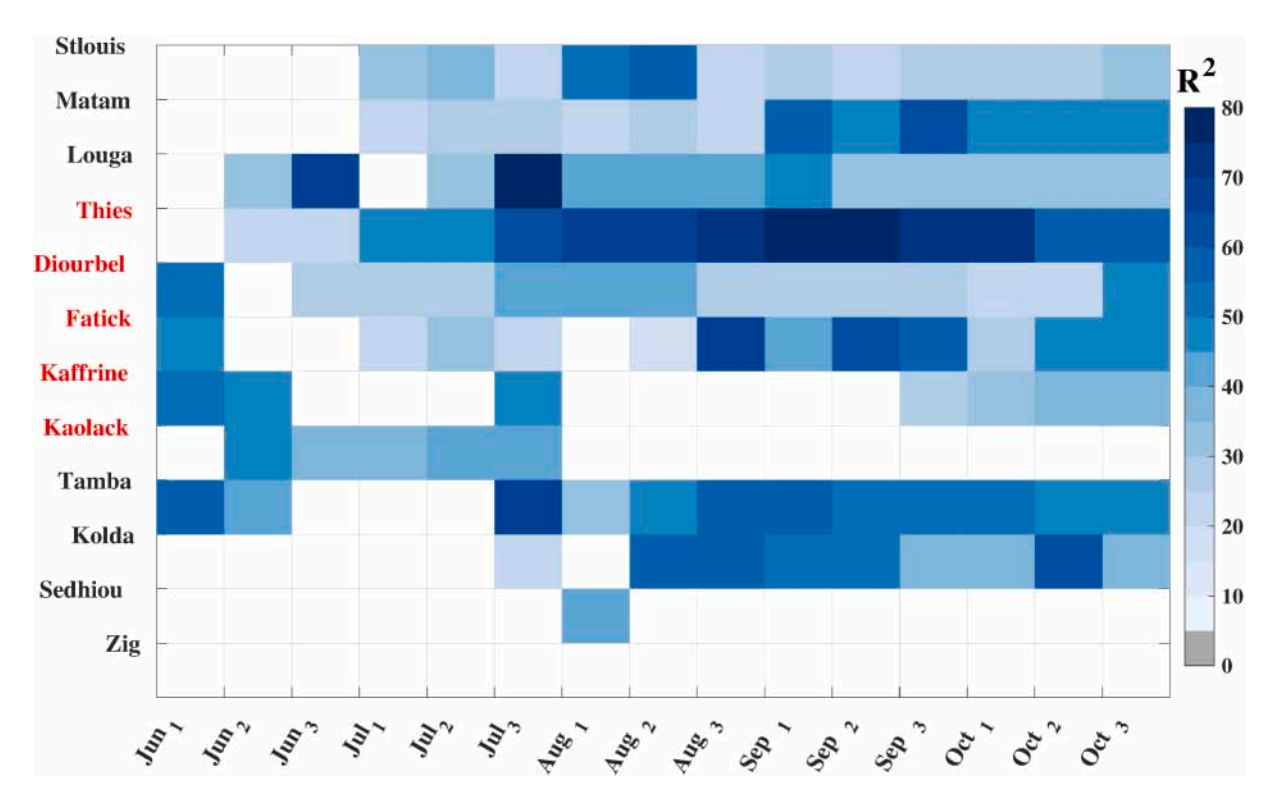


Fig. 7. Portrait diagram of best coefficient of determination R² in each dekad from June to October for all models tested. These 5 regions (in red) Thies, Kaffrine, Kaolack, Fatick and Diourbel reflect the groundnut basin with more than 70% of the national production. White pixels are associated to non-significant relationship.

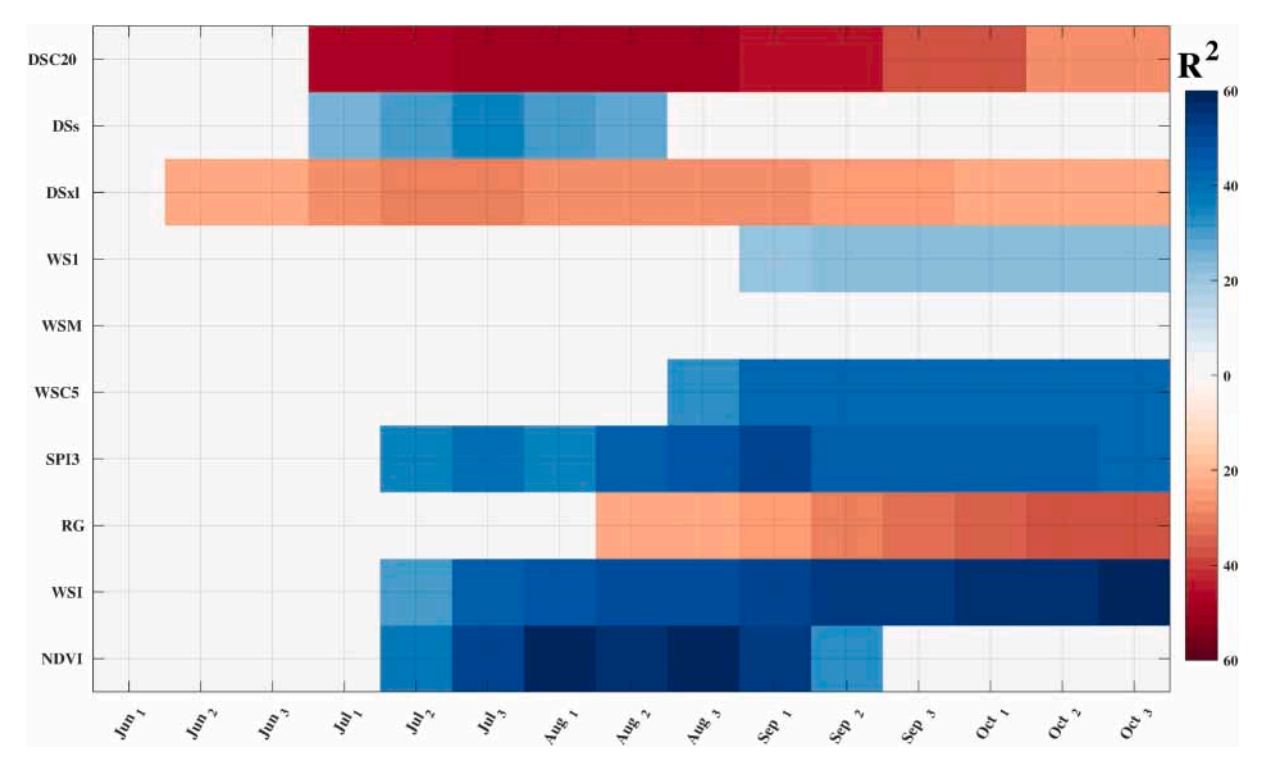


Fig. 8. Portrait diagram of slope provided by dry/wet spells and remote sensing indicators for each dekad in Thies. The shaded colour represent the R² score in the first and second phase of the protocol. Red color indicates negative slope and blue color positive slope.

4.5. Yields estimated by the model

The accuracy of the prediction increases during the season as more information about the season and in particular its rainfall distribution becomes available: In early July, August, September and October, respectively 48, 69, 79 and 72% of millet yield variability could be explained by the best combination of indicators (Fig. 12). The evolution of the correlations of dry spells indicators with yields (Fig. 12a) suggests that dry spells occurring during crop emergence – early development have an impact on final yield (see R² of DSC20 and DSs from early July to mid August; DSxl starts in mid June and reaches a plateau in July, mainly because DSxl occur at the start of season – see Fig. S3 in supplementary material). This observation agrees with the observation that young plants are sensitive to prolonged dry spells (Del Rio and Simpson, 2014). Wet spells tend to influence yields in the middle or end of the season (as from end of August early September) with a positive slope. This suggests that wet spells did not cause damage to crops at the scale of the region, but on the contrary favoured the crop during the grain filling phase, another sensitive phase for millet (Del Rio and Simpson, 2014). The remote sensing indicators also have a response that varies in the season (Fig. 9b). The influence of NDVI increases from mid July to August then decreases rapidly while that of cumulated RG grows throughout the season. SPI3 and WSI have strong information at the beginning of the season but then tend to stabilize. Finally, the model shows some limitations in extreme agronomic years such as 2002, 2004, 2007 (low yields) and 1995, 2010 (high yields). During low yield years (2002 and 2004) an overestimation of yields close to 100 kg/ha was observed although this gap narrowed in 2007. The temporal resolution of the predictor (dekad) may explain the decrease in model performance as the duration of these events ranges from 1 day (WS1) to more than 15 days (DSxl, DSC20). Furthermore, during the years with the highest millet yields (1995; 2008; 2009; 2010), the model tends to underestimate the final yield at the beginning of the season. At the end of the season, the predicted yields are more accurate.

5. Discussion

Inter-annual variability of crop yields is well known to depend on climatic factors especially in semi arid regions (Chen et al., 2004). The consensus is that rainfall appears to be the direct cause of year-to-year variability of crop yields in the Sahel (Gunning and Collier, 1999; Guan et al., 2015; Sultan and Gaetani, 2016). However, the accumulation of seasonal rainfall is often insufficient to explain variations in the agricultural yields because these latter are mainly sensitive to rainfall intraseasonal distribution (Feng et al., 2018; Cai et al., 2017). In our study, dry and wet spells proposed as key descriptors of the intra seasonal rainfall variability appear to improve the prediction of millet yields when combined with other indicators in the CST model. The 12 regions of Senegal have been studied independently. We obtained the highest agreement between observed and predicted yields ($R^2 = 60-80\%$) in the region of Thies by including dry and wet spells as covariates in the model. There are the large disparities of the performance between the regions even under the same climatology, such as the groundnut basin. We are not able to provide explanations to explain these differences.

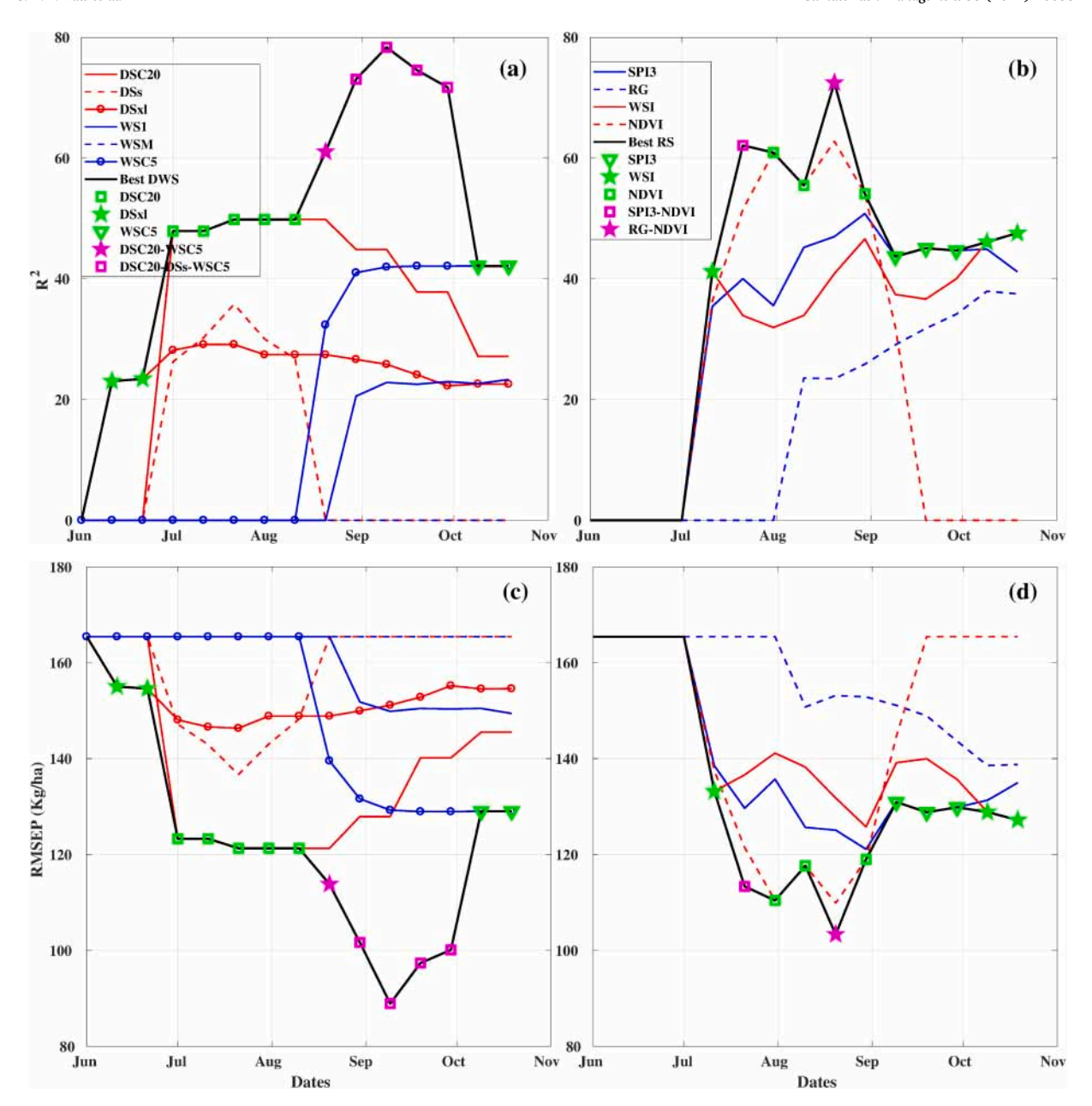


Fig. 9. Coefficient of determination (R^2) and Root mean squared error of prediction (RMSEP) through the season (JJASO) with runs combined dry and wet spell (first column) and combined remote sensing ((first column)) in Thies. The black line represents the best combinations of dry/wet spells (DWS) and remote sensing indicators (RS) for each dekad. Symbols represent the best indicator (green) or Indicators combined (magenta) for each dekad.

Nevertheless, the results can be compared to previous studies. Several results focusing on climate variability and crop production in Sahel seem to be in line with our finding. Rasmussen (1999) found that 88% of the variation in millet yield is explained by NDVI combined with other environmental parameters in sahel. Leroux et al. (2016) found similar scores using a combination of NDVI and Land Surface Temperature ($R^2 = 0.67$) indices, which clearly outperformed the model based on NDVI alone ($R^2 = 0.34$). The scores are higher than those based only on absolute rainfall amounts in West Africa (e.g. $R^2 = 35\%$ in Berg et al. (2010)) and close to those obtained in other regions of the world with comparable dry and wet spells indicators such as Feng et al. (2018) in Australia with R^2 scores ranging from 34 to 58%. The other major advantage of dry spells is that they allow an early forecast of millet yield in the rainy season. The beginning of significant predictability by using DS end June early July are earlier than those found by Mounkaila et al. (2019) who estimate that the earliest forecast for millet in Niger is for the third dekad of July. Moreover, a strong spatial disparity in the performance of the indicators has been highlighted in this study. Over Southern Senegal, wet spells and RG seem to be more efficient in early September. Finally, we also showed that DSC20 occurring in the early vegetative development determines final yields,

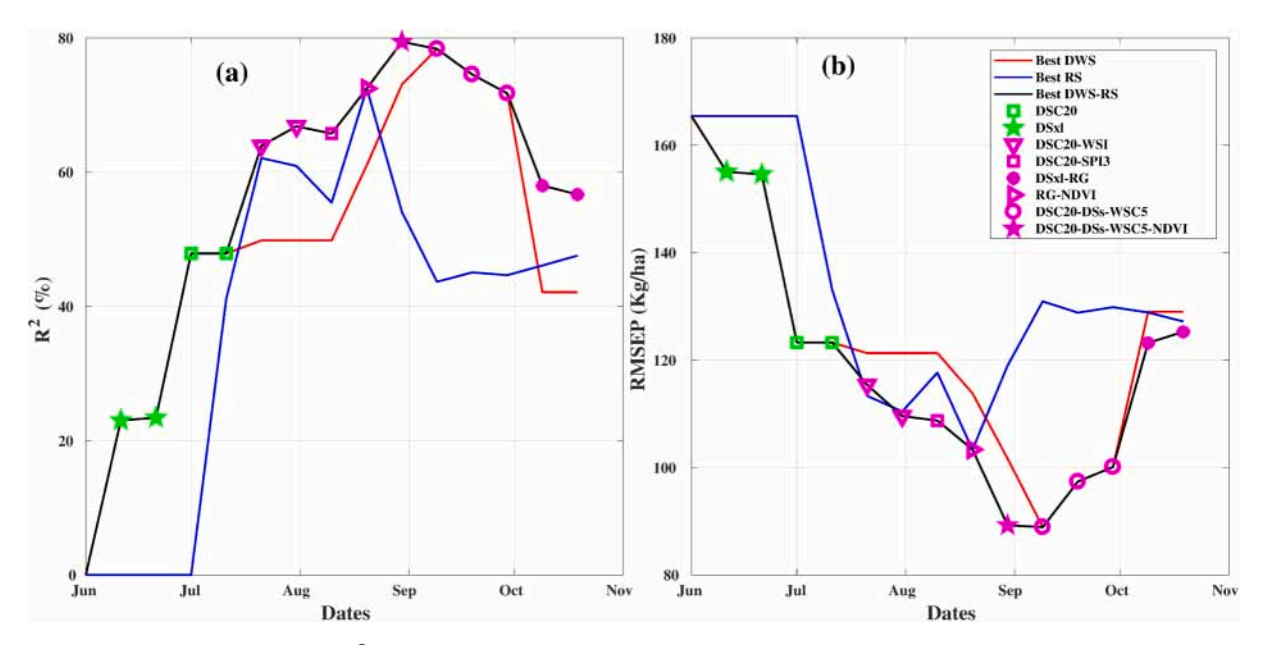


Fig. 10. Coefficient of determination (R²) and Root mean squared error of prediction (RMSEP) through the season (JJASO) with runs combined dry/wet spell and remote sensing in Thies. The black line represents the best combinations of dry/wet spells and remote sensing indicators (Best DWS-RS). Symbols represent the best indicator (green) or Indicators combined (magenta) for each dekad.

these results corroborate findings of Gibon et al. (2018).

Focussing on Thies, the region in the groundnut basin with the highest predictability, we showed that most indicators depict relations with yield with a sign of correlation (positive or negative) in general consistent with the expected effect of the indicator. The first exception is the negative correlation with cumulated RG. That is related to the link between the increase of clouds (and so potentially rainfall) and the decrease of RG in a tropical region where the solar radiation is not a limited factor. Dry spells are negatively correlated with yield. This is in line with Laudien et al. (2020) who found that occurrence of consecutive dry days of more than 5 days (cdd5) are mostly negatively correlated with yields, in particular in the vegetative phase in Tanzania. Our results show no significant negative effects of wet spells on production in Thies, and instead a positive counterintuitive impact of WS1 and WSM is observed (Fig. 8). A possible explanation is that the thresholds used are not high enough to be considered as extreme (from 20 mm.day-1 in the North to 65 mm.day-1 in the South, Fig. S9). Indeed, a percentile method has been adopted to select a robust number of events over all the country. It is possible that these values are lower than the sensitivity of yields to rainfall over most of the agricultural regions of the basin and in the north of the country. On the contrary, the wet spells that are detected in the basin may correspond in most cases to moderate rainfall (30 and 40 mm per. day-1 in the basin, Fig. S4 in supplementary material), which is favourable to millet yields. These results may also be due to the spatial dimension of these disasters. While drought affects large areas (Lesk et al., 2016), floods are generated by the convective part of MCSs and can be very localised (Engel et al., 2017). As this study uses agricultural statistics at the regional level, it can be assumed that a flooding effect is more perceptible on finer spatial scales.

It is noteworthy that our study provides robust scores, nevertheless, providing an early forecast of yields for the main producing regions is still a challenge. This is especially due to several sources of uncertainties related to our statistical models. Firstly, the quality of yield statistics may be biased due to different reasons; the sampling protocol (e.g. based on an outdated list of farmers), lack of means to perform the survey, the type of survey (based on objective measurements or on reported yields), and some risk of manipulation. Indicators derived from satellite images or ground observations may also be inaccurate. Indeed, the density of the raingauge network is coarse and its spatial distribution is heterogeneous. These characteristics can clearly affect the spatialisation of rainfall and thus the detection of dry and wet spells. Ali et al. (2005) drew our attention to this point by demonstrating that the estimation error increases from south to north and remains below 10% for the area south of 15°N and west of 11°E (covering Senegal). In the southern Sahel (south of 15°N), the rain gauge density needs to be at least 10 gauges per 2.5° 2.5° grid cell for a monthly error of less than 10%. In the northern Sahel, this density increases to more than 20 gauges because of the large intermittency of rainfall. The remote sensing indicators are derived through algorithms based on assumptions (e.g. SPI-3 or WSI are derived from CHIRPS rainfall estimates) and may contain inaccuracy. Fall et al. (2021) has found the number of dry and wet spells is highly dependent on the rainfall product used and their uncertainties. The NDVI data come from NOAA AVHRR satellites, which for NOAA-11 had a strong time drift between 1989 and 1994. Surprisingly at the end of September, i.e. the time of maximum biomass, the four lowest NDVI values for Thies are recorded on years 1991, 1992, 1993 and 1994 (Fig. S5 of supplementary material). The fact that only 1992 and 1991 had low seasonal rainfall according to SPI3 and the Lamb index from gauge data (BK), of the four years, only 1992 had a severe drought) suggests a bias issue with the AVHRR sensor. Actually NOAA 11, which covered years 1991 to 1994 in our time series, is known for having had a strong time drift in its overpass time, which resulted in an NDVI decrease with the increase in solar zenith angle (Privette et al., 1995). The second

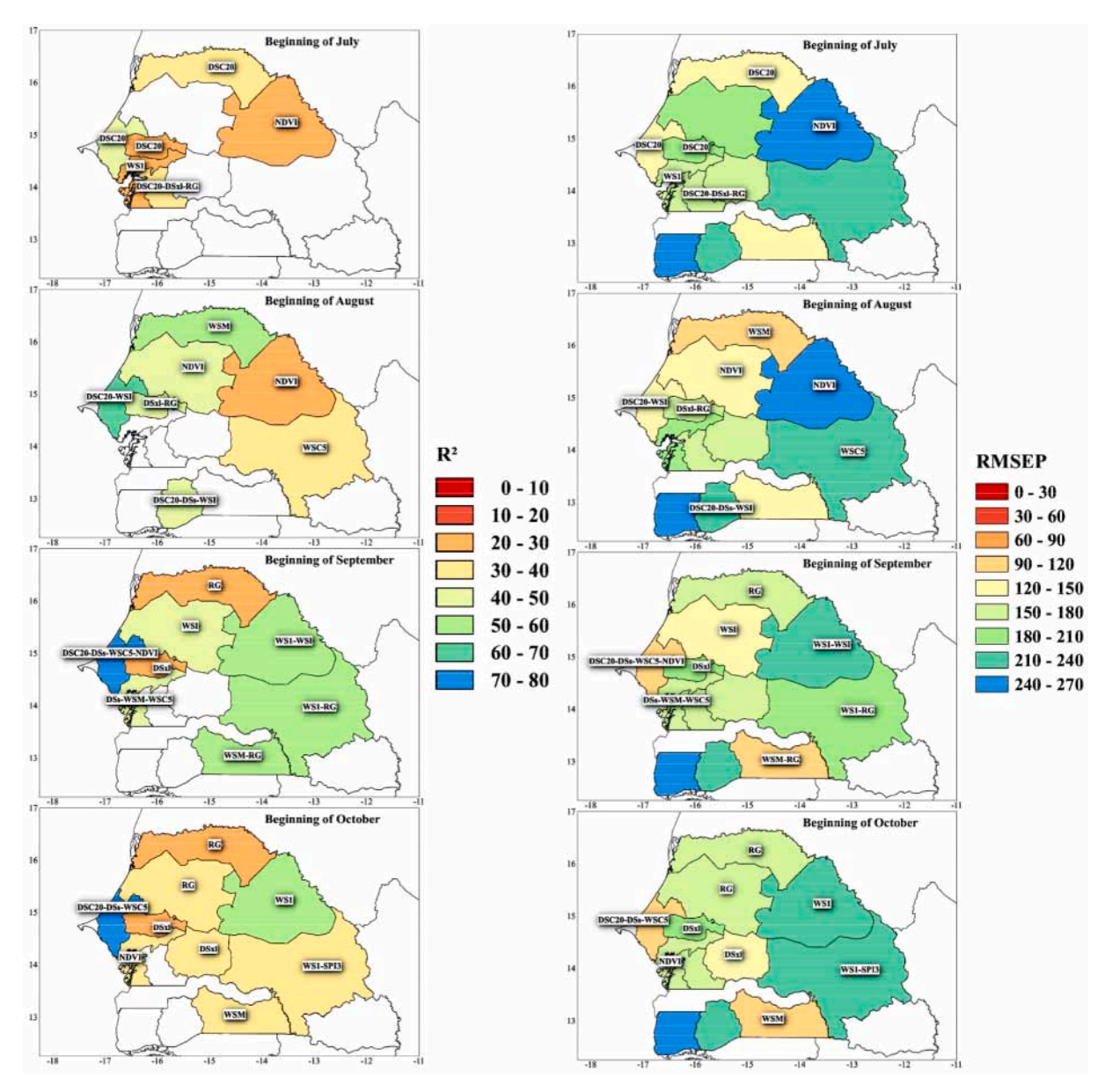


Fig. 11. Spatial distribution of R² of best predictors from July to October for each region in Senegal over 1991–2010 period column) and the RMSEP (second column). Labels represent the name of the best predictor in the region.

source of uncertainties is related to the MLR itself. Indeed, MLR assumes linear effects between the indicators and yield. Moreover all the indicators are somehow correlated to water stress, so the selection of one indicator rather than another may be the result of chance. Our study is quite exposed to multicollinearity when we combine the indicators, and one index might mask the contribution from another (Chatterjee and Hadi, 2012). However, this does not affect the capacity of the MLR model to obtain a good fit with yield data, or to perform good predictions (Dielman, 2005). To model nonlinear processes, algorithms like random forest could be used. Finally, the last uncertainty is related to the link between identified predictors and yields. Our predictors are mainly related to lack and excess of rainfall over the season or biomass in the case of NDVI. Other factors affecting yields (e.g. insects or diseases, excessive temperature e.g. at flowering) are clearly not taken into account in our models. Also, even if wet spells are considered, the effect of excess rainfall at flowering has not been captured from our training data (as shown by the positive slope with wet spells).

6. Conclusions

This study analyses the impacts and potential operational interest of integrating various dry and wet periods indicators to remote sensing indicators (NDVI, RG, WSI and SPI-3) to predict millet yields in Senegal using a multiple linear regression model through the

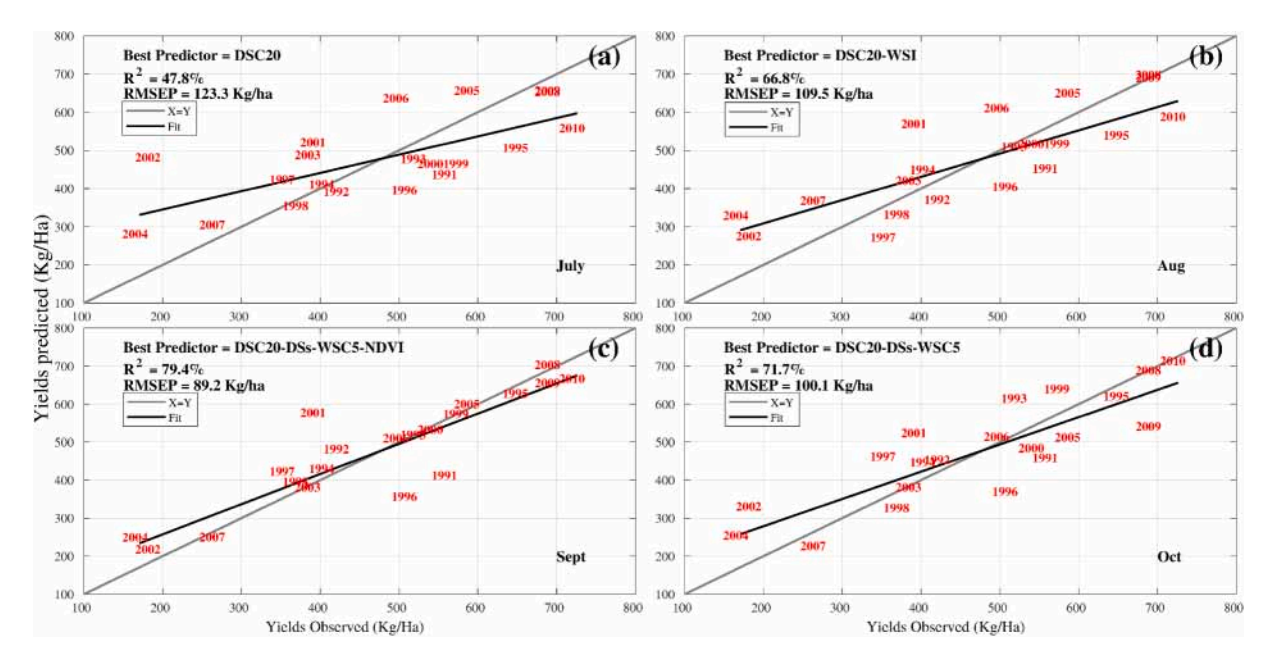


Fig. 12. Comparison between observed DAPSA yields and model-estimated yields in early July, early August, early September and early October with the R² and RMSEP predictor through scatter plot for the years 1991 to 2010 in Thies.

CST tool. In view of the emergence of more frequent extreme rainfall events during the summer season as a new threat to rainfed farming systems, new climate information services and indicators for food security in the region are needed. Our results showed that WS1 and WSC5 are positively correlated with yields, whereas the occurrence of dry spells are mostly negatively correlated with yield except DSs. DSC20 plays an important role in explaining millet yield variability. Among all the regions, Thies (region in the peanut bassin located at western-center of Senegal- see Fig. 1 and 2) appears as the best region for predicting millet yields with our indicators. In this region, combining dry and wet spells with remote sensing indicators explains more than 80% of the millet yield variability. Early season DSC20 and the July NDVI are identified as the most important indicators. The best prediction performance is achieved as early as the first dekad of September with the DSC20-DSs-WSC5-NDVI combination, while final production estimates are generally available a few months after harvest, which usually finishes around November (Jacques and Defourny, 2019). The results also show that dry and wet spell indicators are linked to yield during the early and mid-season. At the end of the season (i.e. October) these indicators have less skill to forecast yield. This earlier warning than the previous version of the model would greatly improve the effectiveness of policy responses to food shortages. The framework applied in this study is a first step to further research on the inter-annual variability of yield in the context of early warning at inter-annual time scale.

This study provided a vulnerability map of dry and wet spells combined with remote sensing indicators impacts that showed peanut basin as a high risk area. Despite the fact that the season begins in the South, while evolving in the North, prediction is more efficient in the peanut basin located at western center of the country. However, we have shown that the model performs consistently well in September. We compared the observed and predicted yields during the rainy season. Our results showed that despite more information about the season accumulated at the end of the season, predictions can get some skills at the beginning of the rainy season (June). Nevertheless, the linear regression model approach reaches its limit during extreme years, when the model is not able to match observations. Therefore, future work could consider using machine learning algorithms such as random forest (Jeong et al., 2016; Feng et al., 2018). The ability of machine learning methods to investigate nonlinear and hierarchical relationships between the predictors and the response using an ensemble learning approach could significantly improve predictions. For example, it could improve the precision of climate-yield relationship diagnostics, overcome the shortcomings of linear regressions models in dealing with correlated predictors, and reveal new insights into different effects of similar climate factors on crop yields.

Declaration of Competing Interest

The authors declare that they have no known competing financial interests or personal relationships that could have appeared to influence the work reported in this paper.

Acknowledgement

The research leading to these results has received funding from the NERC/DFID Future Climate for Africa programme under the AMMA-2050 project, Grant NE/M020428/2.

Appendix A. Supplementary data

Supplementary data associated with this article can be found, in the online version, athttps://doi.org/10.1016/j.crm.2021.100331.

References

Abbam, T., Amoako Johnson, F., Dash, J., Padmadas, S., 2018. Spatiotemporal variations in rainfall and temperature in ghana over the twentieth century, 1900–2014. Earth Space Sci. 5.https://doi.org/10.1002/2017EA000327.

Ajetomobi, J., 2016. Effects of weather extremes on crop yields in nigeria. Afr. J. Food Agric. Nutr. Dev. 16, 11168–11184. https://doi.org/10.18697/ajfand.76.15685.

Alhassane, A., Salack, S., Ly, M., Lona, I., Traore, S., Sarr, B., 2013. Evolution of agro-climatic risks related to the recent trends of the rainfall regime over the sudanosahelian region of west africa. Science et changements planétaires/ Sécheresse 24, 282–293. https://doi.org/10.1684/Section 2013.0400.

Ali, A., Amani, A., Diedhiou, A., Lebel, T., 2005. Rainfall estimation in the sahel. Part ii: Evaluation of rain gauge networks in the cilss countries and objective intercomparison of rainfall products. J. Appl. Meteorol. 44, 1707–1722. https://doi.org/10.1175/JAM2305.1.

Bacci, M., 2017. Characterization of climate risks for rice crop in casamance, senegal. Green Energy Technol. 57-72.

Bamba, B., Gueye, M., Badiane, A., Ngom, D., Samba Laha, K., 2019. Effet de la date et de la densité de semis sur la croissance et le rendement en grain du mil tardif [pennisetum glaucum (l.) r. br] dans les zones sud est et sud du sénégal 138.

Barron, J., Rockström, J., Gichuki, F., Hatibu, N., 2003. Dry spell analysis and maize yields for two semi-arid locations in east africa. Agric. For. Meteorol. 117, 23–37. https://doi.org/10.1016/S0168-1923(03)00037-6.

Berg, A., Sultan, B., de NOBLET, N., 2010. What are the dominant features of rainfall leading to realistic large-scale crop yield simulations in west africa? Geophys. Res. Lett. 37 https://doi.org/10.1029/2009GL041923.

Berry, G.J., Thorncroft, C.D., 2012. African easterly wave dynamics in a mesoscale numerical model: The upscale role of convection. J. Atmos. Sci. 69, 1267–1283. https://doi.org/10.1175/JAS-D-11-099.1. URL: https://journals.ametsoc.org/view/journals/atsc/69/4/jas-d-11-099.1.xml.

Berry, P., Sterling, M., Spink, J., Baker, C., Sylvester-Bradley, R., Mooney, S., Tams, A., Ennos, R., 2004. Understanding and reducing lodging in cereals. Adv. Agron. 84, 217–271. https://doi.org/10.1016/S0065-2113(04)84005-7.

Cai, Y., Moore, K., Pellegrini, A., Elhaddad, A., Lessel, J., Townsend, C., Solak, H., Semret, N., 2017. Crop yield predictions – high resolution statistical model for intraseason forecasts applied to corn in the us.

Chatterjee, S., Hadi, A., 2012. Regression analysis by example, fifth ed. John Wiley & Sons Inc., Hoboken.

Chen, J., Jönsson, P., Tamura, M., Gu, Z., Matsushita, B., Eklundh, L., 2004. A simple method for reconstructing a high-quality ndvi time-series data set based on the savitzky-golay filter. Remote Sens. Environ. 91, 332–344. https://doi.org/10.1016/j.rse.2004.03.014.

Del Rio, A., Simpson, B., 2014. Fifteen crop phenological profiles for climate change adaptation.

Descroix, L., Diongue Niang, A., Panthou, G., Bodian, A., Sane, Y., Dacosta, H., Malam Abdou, M., Vandervaere, J.-P., Quantin, G., 2016. Évolution récente de la pluviométrie en afrique de l'ouest á travers deux régions: la sénégambie et le bassin du niger moyen. Climatologie 12, 25–43. https://doi.org/10.4267/climatologie.1105.

Diagne, A., Cabral, F.J., 2017. Agricultural transformation in senegal: Impacts of an integrated program. https://doi.org/10.2139/ssrn.3163680.

Diedhiou, A., Janicot, S., Viltard, A., Felice, P., 1998. Evidence of two regimes of easterly waves over west africa and tropical atlantic. Geophys. Res. Lett. 25, 2805–2808. https://doi.org/10.1029/98GL02152.

Dielman, T., 2005. Applied regression analysis: a second course in business and economic statistics., Brooks-Cole Thomson Learning (2005). Pacific Grove.

Dieng, O., Roucou, P., Louvet, S., 2008. Variabilité intra-saisonnière des précipitations au sénégal (1951-1996).

Dingkuhn, M., Singh, B., Clerget, B., Chantereau, J., Sultan, B., 2006. Past, present and future criteria to breed crops for water-limited environments in west africa. Agric. Water Manag. 80, 241–261. https://doi.org/10.1016/j.agwat.2005.07.016.

Dione, C., Lothon, M., Daouda, B., Campistron, B., Couvreux, F., Guichard, F., Sall, S.M., 2014. Phenomenology of sahelian convection observed in niamey during the early monsoon. Q. J. R. Meteorol. Soc. 140 https://doi.org/10.1002/qj.2149.

Diongue, A., Lafore, J.-P., Redelsperger, J.-L., Roca, R., 2002. Numerical study of a sahelian synoptic weather system: Initiation and mature stages of convection and its interactions with the large-scale dynamics. Q. J. R. Meteorol. Soc. 128, 1899–1927. https://doi.org/10.1256/003590002320603467.

Diop, L., Bodian, A., Diallo, D., 2016. Spatiotemporal trend analysis of the mean annual rainfall in senegal. Eur. Scientific J. 12, 231. https://eujournal.org/index.php/esj/article/view/7300.https://doi.org/10.19044/esj.2016.v12n12p231.

Dong, B., Sutton, R., 2015. Dominant role of greenhouse-gas forcing in the recovery of sahel rainfall. Nat. Clim. Change 5. https://doi.org/10.1038/nclimate2664. Eerens, H., Haesen, D., Rembold, F., Urbano, F., Tote, C., Bydekerke, L., 2014. Image time series processing for agriculture monitoring. Environ. Model. Software 53, 154–162. https://doi.org/10.1016/j.envsoft.2013.10.021. URL: http://www.sciencedirect.com/science/article/pii/S1364815213002648.

Engel, T., Fink, A.H., Knippertz, P., Pante, G., Bliefernicht, J., 2017. Extreme precipitation in the west african cities of dakar and ouagadougou: atmospheric dynamics and implications for flood risk assessments. J. Hydrometeorol. 18, 2937–2957. https://doi.org/10.1175/JHM-D-16-0218.1.

Fall, C.M.N., Lavaysse, C., Drame, M.S., Panthou, G., Gaye, A.T., 2021. Wet and dry spells in Senegal: comparison of detection based on satellite products, reanalysis, and in situ estimates. Nat. Hazards Earth Syst. Sci. 21, 1051–1069. https://doi.org/10.5194/nhess-21-1051-2021.

Feng, P., Wang, B., Xing, H., Ji, F., Macadam, I., Ruan, H., Yu, Q., 2018. Impacts of rainfall extremes on wheat yield in semi-arid cropping systems in eastern australia. Clim. Change 147, 555–569. https://doi.org/10.1007/s10584-018-2170-x.

Frere, M., Popov, G., 1986. Early agrometeorological crop yield assessment. Food Agric. Organization United Nations 73, 144.

Froidurot, S., Diedhiou, A., 2017. Characteristics of wet and dry spells in the west african monsoon system. Atmospheric Sci. Lett. 18 https://doi.org/10.1002/asl.734. Funk, C., Peterson, P., Landsfeld, M., Pedreros, D., Verdin, J., Shukla, S., Husak, G., Rowland, J., Harrison, L., Hoell, A., Michaelsen, J., 2015. The climate hazards infrared precipitation with stations – a new environmental record for monitoring extremes. Scientific Data 2, 150066. https://doi.org/10.1038/sdata.2015.66.

Ganyo, K., Muller, B., Koudjo Espoir, G., Guisse, A., Cisse, N., Adam, M., 2018. Optimisation du npk et urée basée sur les informations climatiques pour accroître la production du sorgho en zone soudano-sahélienne du sénégal. J. Appl. Biosci. 131, 13293–13307. https://doi.org/10.4314/jab.v131i1.5.

Giannini, A., 2015. Hydrology: Climate change comes to the sahel. Nat. Clim. Change 5, 720-721. https://doi.org/10.1038/nclimate2739.

Gibon, F., Pellarin, T., Román-Cascón, C., Alhassane, A., Traoré, S., Kerr, Y., Lo Seen, D., Baron, C., 2018. Millet yield estimates in the sahel using satellite derived soil moisture time series. Agric. For. Meteorol. 262, 100–109. https://doi.org/10.1016/j.agrformet.2018.07.001.

Giorgi, F., Im, E.-S., Coppola, E., Diffenbaugh, N.S., Gao, X.J., Mariotti, L., Shi, Y., 2011. Higher hydroclimatic intensity with global warming. J. Clim. 24, 5309–5324. https://doi.org/10.1175/2011JCLI3979.1.

Goedhart, P., Steven, H., Boogaard, H., 2017. The cgms statistical tool user manualv 3, 69-71.

Grillot, M., 2018. Modélisation multi-agents et pluri-niveaux de la réorganisation du cycle de l'azote dans des systèmes agro-sylvo-pastoraux en transition – le cas du bassin arachidier au sénégal.

Grodsky, S., Carton, J., 2001. Coupled land/atmosphere interactions in the west african monsoon. Geophys. Res. Lett. 28, 1503–1506. https://doi.org/10.1029/2000GL012601.

Guan, K., Sultan, B., Biasutti, M., Baron, C., Lobell, D., 2015. What aspects of future rainfall changes matter for crop yields in west africa? Geophys. Res. Lett. 42 https://doi.org/10.1002/2015GL063877 n/a-n/a.

Gunning, J., Collier, P., 1999. Why has africa grown slowly? J. Econ. Perspect. 13, 3-22. https://doi.org/10.1257/jep.13.3.3.

- Innes, P., Tan, D., Van Ogtrop, F., Amthor, J., 2015. Effects of high-temperature episodes on wheat yields in new south wales, australia. Agric. For. Meteorol. 208, 95–107. https://doi.org/10.1016/j.agrformet.2015.03.018.
- Isaaks, E., Srivaski, R., 2020. Block kriging 323-331.
- Islam, 1992. Influence of solar radiation and temperature on irrigated rice grain yield in bangladesh. Field Crops Res. 30, 13–28.https://doi.org/10.1016/0378-4290 (92)90053-C.
- Jacques, D., Defourny, P.. 2019. Accuracy requirements for early estimation of crop production in senegal.
- Janicot, S., Caniaux, G., Chauvin, F., de coetlogon, G., Fontaine, B., Hall, N., Kiladis, G., Lafore, J.-P., Lavaysse, C., Lavender, S., Leroux, S., Marteau, R., Mounier, F., Philippon, N., Roehrig, R., Sultan, B., Taylor, C., 2011. Monsoon multidisciplinary analysis (amma): an integrated project for understanding of the west african climate system and its human dimension.
- Janicot, S., Caniaux, G., Chauvin, F., de Coëtlogon, G., Fontaine, B., Hall, N., Kiladis, G., Lafore, J.-P., Lavaysse, C., Lavender, S.L., Leroux, S., Marteau, R., Mounier, F., Philippon, N., Roehrig, R., Sultan, B., Taylor, C.M., 2011. Intraseasonal variability of the west african monsoon. Atmos. Sci. Lett. 12, 58–66. https://doi.org/10.1002/asl.280.
- Jenkins, G., Kucera, P., Joseph, E., Fuentes, J., Gaye, A., Gerlach, J., Roux, F., Viltard, N., Papazzoni, M., Protat, A., Bouniol, D., Reynolds, A., Arnault, J., Daouda, B., Kébé, C., Camara, M., Sall, S., Ndiaye, S., Deme, A., 2010. Coastal observations of weather features in senegal during the african monsoon multidisciplinary analysis special observing period 3. J. Geophys. Res. 115 https://doi.org/10.1029/2009JD013022.
- Jeong, J.H., Resop, J.P., Mueller, N.D., Fleisher, D.H., Yun, K., Butler, E.E., Timlin, D.J., Shim, K.-M., Gerber, J.S., Reddy, V.R., Kim, S.-H., 2016. Random forests for global and regional crop yield predictions. PLOS ONE 11, 1–15. https://doi.org/10.1371/journal.pone.0156571. DOI: 10.1371/journal.pone.0156571.
- Kerdiles, H., Rembold, F., Leo, O., Boogaard, H., Hoek, S., 2017. Cst, a freeware for predicting crop yield from remote sensing or crop model indicators. In: Illustration with rsa and ethiopia, pp. 1–6. https://doi.org/10.1109/Agro-Geoinformatics.2017.8047071.
- Kumar, M., Murthy, C., Seshasai, M., Roy, P., 2009. On the use of standardized precipitation index (spi) for drought intensity assessment. Meteorl. Appl. 16, 381–389. https://doi.org/10.1002/met.136.
- Lafore, J.-P., Flamant, C., Giraud, V., Guichard, F., Knippertz, P., Mahfouf, J.-F., Mascart, P., Williams, E., 2010. Introduction to the amma special issue on 'advances in understanding atmospheric processes over west africa through the amma field campaign'. Q. J. R. Meteorol. Soc. 136.
- Lafore, J.-P., Beucher, F., Peyrillé, P., Diongue-Niang, A., Chapelon, N., Bouniol, D., Caniaux, G., Favot, F., Ferry, F., Guichard, F., Poan, D., Roehrig, R., Vischel, T., 2017. A multi-scale analysis of the extreme rain event of ouagadougou in 2009. Q. J. R. Meteorol. Soc. https://doi.org/10.1002/qj.3165.
- Lalou, R., Sultan, B., Muller, B., Ndonky, A., 2019. Does climate opportunity facilitate smallholder farmers' adaptive capacity in the sahel? Palgrave Commun. 5 https://doi.org/10.1057/s41599-019-0288-8.
- Laudien, R., Schauberger, B., Makowski, D., Gornott, C., 2020. Robustly forecasting maize yields in tanzania based on climatic predictors. Scientific Rep. 10 https://doi.org/10.1038/s41598-020-76315-8.
- Laurent, H., D'Amato, N., Lebel, T., 1998. How important is the contribution of mesoscale convective complexes to the sahelian rainfall. Phys. Chem. Earth 23, 629–633. https://doi.org/10.1016/S0079-1946(98)00099-8.
- Lavaysse, C., Diedhiou, A., Laurent, H., Lebel, T., 2006. African easterly waves and convective activity in wet and dry sequences of the west african monsoon. Clim. Dyn. 27, 319–332. https://doi.org/10.1007/s00382-006-0137-5.
- Lavaysse, C., Flamant, C., Evan, A., Janicot, S., Gaetani, M., 2016. Recent climatological trend of the saharan heat low and its impact in west african climate. Clim. Dyn. 47 https://doi.org/10.1007/s00382-015-2847-z.
- Lavaysse, C., Vogt, J., Toreti, A., Carrera, M., Pappenberger, F., 2018. On the use of weather regimes to forecast meteorological drought over europe. Nat. Hazards Earth Syst. Sci. 18, 3297–3309. https://doi.org/10.5194/nhess-18-3297-2018.
- Lavender, S.L., Matthews, A.J., 2009. Response of the west african monsoon to the madden-julian oscillation. J. Clim. 22, 4097–4116.https://journals.ametsoc.org/view/journals/clim/22/15/2009jcli2773.1.xml.https://doi.org/10.1175/2009JCLI2773.1.
- Le Barbé, L., Lebel, T., Tapsoba, D., 2002. Rainfall variability in west africa during the years 1950–90. J. Clim. 15, 187–202. https://doi.org/10.1175/1520-0442
- Lebel, T., Ali, A., 2009. Recent trends in the central and western sahel rainfall regime (1990–2007). J. Hydrol. 375, 52–64. https://doi.org/10.1016/j.ihydrol.2008.11.030.
- Lebel, T., Diedhiou, A., Laurent, H., 2003. Seasonal cyle and interannual variability of the sahelian rainfall at hydrological scales.
- Leroux, L., Baron, C., Zoungrana, B., Traore, S., Lo Seen, D., Bégué, A., 2016. Crop monitoring using vegetation and thermal indices for yield estimates: Case study of a rainfed cereal in semi-arid west africa. IEEE J. Sel. Top. Appl. Earth Observ. Remote Sens. 9, 347–362. https://doi.org/10.1109/JSTARS.2015.2501343.
- Lesk, C., Rowhani, P., Ramankutty, N., 2016. Influence of extreme weather disasters on global crop production. Nature 529, 84–87. https://doi.org/10.1038/
- Li, J., Lewis, J., Rowland, J., Tappan, G., Tieszen, L., 2004. Evaluation of land performance in senegal using multi-temporal ndvi and rainfall series. J. Arid Environ. 59 https://doi.org/10.1016/j.jaridenv.2004.03.019.
- Lloyd, C., Atkinson, P., 2001. Assessing uncertainty in estimates with ordinary and indicator kriging. Comput. Geosci. 27, 929–937. https://doi.org/10.1016/S0098-3004(00)00132-1.
- Lobell, D.B., Burke, M.B., 2010. On the use of statistical models to predict crop yield responses to climate change. Agric. For. Meteorol. 150, 1443–1452. https://doi.org/10.1016/j.agrformet.2010.07.008. URL: http://www.sciencedirect.com/science/article/pii/S0168192310001978.
- Lobell, D., Burke, M., Tebaldi, C., Mastrandrea, M., Falcon, W., Naylor, R., 2008. Prioritizing climate change adaptation needs for food security in 2030. Science (New York, N.Y.) 319, 607–10.https://doi.org/10.1126/science.1152339.
- Maidment, R., Grimes, D., Allan, R., Greatrex, H., Rojas, O., Leo, O., 2013. Evaluation of satellite-based and model re-analysis rainfall estimates for uganda. Meteorol. Appl. 20 https://doi.org/10.1002/met.1283.
- Mathon, V., Laurent, H., Lebel, T., 2002. Mesoscale convective system rainfall in the sahel. J. Appl. Meteorol. 41, 1081–1092. https://doi.org/10.1175/1520-0450 (2002)041<1081:MCSRIT>2.0.CO;2.
- McKee, T.B., 1993. The relationship of drought frequency and duration of time scales. Eighth Conference on Applied Climatology, January, Anaheim, California 1993, 17–22 https://ci.nii.ac.jp/naid/10027618105/en/.
- Meehl, G., Zwiers, F., Evans, J., Knutson, T., Mearns, L., Whetton, P., 2000. Trends in extreme weather and climate events: Issues related to modeling extremes in projections of future climate change. Bull. Am. Meteorol. Soc. 81, 427–436. https://doi.org/10.1175/1520-0477(2000)081<0427:TIEWAC>2.3.CO;2.
- Moriondo, M., Giannakopoulos, C., Bindi, M., 2011. Climate change impact assessment: The role of climate extremes in crop yield simulation. Clim. Change 104, 679–701. https://doi.org/10.1007/s10584-010-9871-0.
- Mounier, F., Janicot, S., 2004. Evidence of two independent modes of convection at intraseasonal timescale in the west african summer monsoon. Citation: Mounier 31. https://doi.org/10.1029/2004GL020665.
- Mounier, F., Janicot, S., Kiladis, G., 2008. The west african monsoon dynamics. Part iii: The quasi-biweekly zonal dipole. J. Clim. 21 https://doi.org/10.1175/2007JCIJ1706.1.
- Mounkaila, Y., Garba, I., Moussa, B., 2019. Yield prediction under associated millet and cowpea crops in the sahelian zone. Afr. J. Agric. Res. 14, 1613–1620. https://doi.org/10.5897/AJAR2019.14225.
- Nain, A.S., Dadhwal, V.K., Singh, T.P., 2004. Use of ceres-wheat model for wheat yield forecast in central indo-gangetic plains of india. J. Agric. Sci. 142, 59–70. https://doi.org/10.1017/S0021859604004022.
- Ndiaye, A., Ousmane, N., Bamba, B., Gueye, M., Sawané, O., 2019. Effets de la fertilisation organo- minérale sur la croissance et le rendement du mil sanio (pennisetum glaucum l. r. br) en haute casamance (sénégal). Eur. Scientific J. 15 https://doi.org/10.19044/esj.2019.v15n33p155.
- Nicholson, S., 2013. The west african sahel: A review of recent studies on the rainfall regime and its interannual variability. ISRN Meteorol. 2013 https://doi.org/10.1155/2013/453521.

- Nicholson, S., Davenport, M., Malo, A., 1990. A comparison of the vegetation response to rainfall in the sahel and east africa, using normalized difference vegetation index from noaa avhrr. Clim. Change 17, 209–241. https://doi.org/10.1007/BF00138369.
- Nicholson, S., Tucker, C., Ba, M., 1998. Desertification, drought, and surface vegetation: An example from the west african sahel. Bull. Am. Meteorol. Soc. 79, 815–829. https://doi.org/10.1175/1520-0477(1998)079<0815:DDASVA>2.0.CO;2.
- Nieuwenhuis, G., Wit, A., Kraalingen, D., Diepen, C., Boogaard, H., 2006. Monitoring crop growth conditions using the global water satisfaction index and remote sensing.
- Oosterom, E., Bidinger, F., Mahalakshmi, V., Rao, K., 1996. Effect of water availability pattern on yield of pearl millet in semi-arid tropical environments. Euphytica 89, 165–173. https://doi.org/10.1007/BF00034602.
- Panthou, G., Vischel, T., Lebel, T., 2014. Recent trends in the regime of extreme rainfall in the central sahel. Int. J. Climatol. 34 https://doi.org/10.1002/joc.3984. Panthou, G., Lebel, T., Vischel, T., Quantin, G., Sane, Y., Abdramane, B., Ndiaye, O., Diongue Niang, A., Diopkane, M., 2018. Rainfall intensification in tropical semi-arid regions: The sahelian case. Environ. Res. Lett. 13 https://doi.org/10.1088/1748-9326/aac334.
- Park, J.-Y., Bader, J., Matei, D., 2016. Anthropogenic mediterranean warming essential driver for present and future sahel rainfall. Nat. Clim. Change 6. https://doi.org/10.1038/nclimate3065.
- Perez Hoyos, A., Rembold, F., Kerdiles, H., Gallego Pinilla, F.J., 2017. Comparison of global land cover datasets for cropland monitoring. Remote Sens. 9 https://doi.org/10.3390/rs9111118.
- Poan, D.E., Lafore, J.-P., Roehrig, R., Couvreux, F., 2015. Internal processes within the african easterly wave system. Q. J. R. Meteorol. Soc. 141, 1121–1136. https://doi.org/10.1002/qj.2420.
- Pohl, B., Fauchereau, N., Richard, Y., Rouault, M., Reason, C., 2009. Interactions between synoptic, intraseasonal and interannual convective variability over southern africa. Clim. Dyn. 33, 1033–1050. https://doi.org/10.1007/s00382-008-0485-4.
- Privette, et al., 1995. Effects of orbital drift on advanced very high resolution radiometer products: Normalized difference vegetation index and sea surface temperature. Remote Sens. Environ. 53, 164–171.https://doi.org/10.1016/0034-4257(95)00083-D.
- Rasmussen, M., 1999. Advances in crop yield assessment in the sahel using remote sensing data. Geografisk Tidsskrift 165-170.
- Rembold, F., Atzberger, C., Savin, I., Rojas, O., Dokuchaev, V., 2013. Using low resolution satellite imagery for yield prediction and yield anomaly detection. Remote Sens. 5 https://doi.org/10.3390/rs5041704.
- Rembold, F., Meroni, M., Urbano, F., Csak, G., Kerdiles, H., Perez Hoyos, A., Lemoine, G., Leo, O., Negre, T., 2018. Asap A new global early warning system to detect anomaly hot spots of agricultural production for food security analysis. Agric. Syst. 168 https://doi.org/10.1016/j.agsy.2018.07.002.
- Rosenzweig, C., Iglesias, A., Yang, X., Epstein, P., Chivian, E., 2001. Climate change and extreme weather events; implications for food production, plant diseases, and pests. Global Change Human Health 2, 90–104. https://doi.org/10.1023/A:1015086831467.
- Rosenzweig, C., Elliott, J., Deryng, D., Ruane, A., Müller, C., Arneth, A., Boote, K., Folberth, C., Glotter, M., Khabarov, N., Hermans, K., Piontek, F., Pugh, T., Schmid, E., Stehfest, E., Yang, H., Jones, J., 2013. Assessing agricultural risks of climate change in the 21st century in a global gridded crop model intercomparison. Proc. Natl. Acad. Sci. U.S.A. 111.https://doi.org/10.1073/pnas.1222463110.
- Roudier, P., Muller, B., d'Aquino, P., Roncoli, C., Soumare, M., Batté, L., Sultan, B., 2014. The role of climate forecasts in smallholder agriculture: Lessons from participatory research in two communities in senegal. Clim. Risk Manage. 2, 42–55. https://doi.org/10.1016/j.crm.2014.02.001.
- Sagna, P., Ndiaye, O., Diop, C., Diongue-Niang, A., Corneille, S., 2015. Are recent climate variations observed in senegal in conformity with the descriptions given by the ipcc scenarios? Atmo. Pollut. 227.
- Salack, S., Klein, C., Giannini, A., Sarr, B., Worou, N., Belko, N., Bliefernicht, J., Kunstman, H., 2016. Global warming induced hybrid rainy seasons in the sahel. Environ. Res. Lett. 11, 104008 https://doi.org/10.1088/1748-9326/11/10/104008.
- Sane, Y., Panthou, G., Bodian, A., Vischel, T., Lebel, T., Dacosta, H., Quantin, G., Wilcox, C., Ndiaye, O., Diongue Niang, A., Diop Kane, M., 2018. Intensity-duration-frequency (idf) rainfall curves in senegal. Nat. Hazards Earth Syst. Sci. Discussions 18, 1–30. https://doi.org/10.5194/nhess-18-1849-2018.
- Schwendike, J., Jones, S.C., 2010. Convection in an african easterly wave over west africa and the eastern atlantic: A model case study of helene (2006). Q. J. R. Meteorol. Soc. 136, 364–396. https://doi.org/10.1002/qj.566.
- Sivakumar, M., 1992. Empirical analysis of dry spells for agricultural applications in west africa. J. Clim. 24, 532–539.
- Sultan, B., Gaetani, M., 2016. Agriculture in west africa in the twenty-first century: Climate change and impacts scenarios, and potential for adaptation. Front. Plant Sci. 7 https://doi.org/10.3389/fpls.2016.01262.
- Sultan, B., Janicot, S., Diedhiou, A., 2003. The west african monsoon dynamics. part i: Documentation of intraseasonal variability. J. Clim. 16, 3389–3406. https://doi.org/10.1175/1520-0442(2003)016<3389:TWAMDP>2.0.CO:2.
- Sultan, B., Bella-Medjo, M., Berg, A., Quirion, P., Janicot, S., 2009. Multi-scales and multi-sites analyses of the role of rainfall in cotton yields in west africa. Int. J. Climatol. 30, 58–71. https://doi.org/10.1002/joc.1872.
- Sultan, B., Roudier, P., Quirion, P., 2013. Les bénéfices de la prévision saisonnière pour l'agriculture en afrique de l'ouest. Secheresse 24, 304–313. https://doi.org/10.1684/Section 2013.0398.
- Sy, O., Fofana, A., Cisse, N., Noba, K., Diouf, D., Ndoye, I., Sané, D., Kane, A., Kane, N., Hash, T., Haussman, B., Elwegan, E., 2015. Étude de la variabilité agromorphologique de la collection nationale de mils locaux du sénégal. J. Appl. Biosci. 87, 8030. https://doi.org/10.4314/jab.v87i1.1.
- Taylor, C., Belušić, D., Guichard, F., Parker, D., Vischel, T., Bock, O., Harris, P.P., Janicot, S., Klein, C., Panthou, G., 1982. Frequency of extreme sahelian storms tripled since, in satellite observations. Nature 544 (2017), 475–478. https://doi.org/10.1038/nature22069.
- Tebaldi, C., Lobell, D., 2008. Towards probabilistic projections of climate change impacts on global crop yields. Geophys. Res. Lett. 35 https://doi.org/10.1029/2008GL033423.
- Trenberth, K.E., 2011. Attribution of climate variations and trends to human influences and natural variability. Wiley Interdiscip. Rev.: Clim. Change 2, 925–930. https://doi.org/10.1002/wcc.142.
- Trenberth, K.E., Dai, A., Rasmussen, R.M., Parsons, D., 2003. The changing character of precipitation. Bull. Am. Meteorol. Soc. 84, 1205–1217. https://doi.org/10.1175/BAMS-84-9-1205.
- Trnka, M., Olesen, J., Kersebaum, K., Skjelvag, A., Eitzinger, J., 2011. Agroclimatic conditions in europe under climate change. Glob. Change Biol. 17, 2298–2318. https://doi.org/10.1111/j.1365-2486.2011.02396.x.
- Troy, T., Kipgen, C., Pal, I., 2015. The impact of climate extremes and irrigation on us crop yields. Environ. Res. Lett. 10 https://doi.org/10.1088/1748-9326/10/5/054013.
- Vijayalakshmi, C., Radhakrishnan, R., Nagarajan, M., Rajendran, C., 1991. Effect of solar radiation deficit on rice productivity. J. Agron. Crop Sci. 167, 184–187. https://doi.org/10.1111/j.1439-037X.1991.tb00952.x.
- Vischel, T., Panthou, G., Peyrillé, P., Roehrig, R., Quantin, G., Lebel, T., Wilcox, C., Beucher, F., Budiarti, M., 2019. Tropical extremes: natural variability and trends. Vogel, E., Donat, M., Alexander, L., Meinshausen, M., Ray, D., Karoly, D., Meinshausen, N., Frieler, K., 2019. The effects of climate extremes on global agricultural yields. Environ. Res. Lett. 14 https://doi.org/10.1088/1748-9326/ab154b.
- Wang, J., Price, K., Rich, P., 2001. Spatial patterns of ndvi in response to precipitation and temperature in the central great plains. Int. J. Remote Sens. 22, 3827–3844. https://doi.org/10.1080/01431160010007033.
- WFP, 2018. Wfp senegal country brief, january 2018.
- Wilcox, C., Vischel, T., Panthou, G., Bodian, A., Blanchet, J., Descroix, L., Quantin, G., Cassé, C., Tanimoun, B., Kone, S., 2018. Trends in hydrological extremes in the senegal and niger rivers. J. Hydrol. 566 https://doi.org/10.1016/j.jhydrol.2018.07.063.
- Wu, M.-L., Reale, O., Schubert, S., 2013. A characterization of african easterly waves on 2.5-6-day and 6–9-day time scales. J. Clim. 26, 6750–6774. https://doi.org/10.1175/JCLI-D-12-00336.1.
- Young, H.R., Cornforth, R.J., Gaye, A.T., Boyd, E., 2019. Event attribution science in adaptation decision-making: the context of extreme rainfall in urban senegal. Clim. Develop. 11, 812–824. https://doi.org/10.1080/17565529.2019.1571401.